

Review

Enhanced Permeability and Retention Effect as a Ubiquitous and Epoch-Making Phenomenon for the Selective Drug Targeting of Solid Tumors

Waliul Islam ^{1,2,3}, Takuro Niidome ² and Tomohiro Sawa ^{1,*}

¹ Department of Microbiology, Graduate School of Medical Sciences, Kumamoto University, Kumamoto 860-8556, Japan

² Faculty of Advanced Science and Technology, Kumamoto University, Kumamoto 860-8555, Japan

³ BioDynamics Research Foundation, Kumamoto 862-0954, Japan

* Correspondence: sawat@kumamoto-u.ac.jp; Tel.: +81-96-373-5100; Fax: +81-96-362-8362

Abstract: In 1979, development of the first polymer drug SMANCS [styrene-co-maleic acid (SMA) copolymer conjugated to neocarzinostatin (NCS)] by Maeda and colleagues was a breakthrough in the cancer field. When SMANCS was administered to mice, drug accumulation in tumors was markedly increased compared with accumulation of the parental drug NCS. This momentous result led to discovery of the enhanced permeability and retention effect (EPR effect) in 1986. Later, the EPR effect became known worldwide, especially in nanomedicine, and is still believed to be a universal mechanism for tumor-selective accumulation of nanomedicines. Some research groups recently characterized the EPR effect as a controversial concept and stated that it has not been fully demonstrated in clinical settings, but this erroneous belief is due to non-standard drug design and use of inappropriate tumor models in investigations. Many research groups recently provided solid evidence of the EPR effect in human cancers (e.g., renal and breast), with significant diversity and heterogeneity in various patients. In this review, we focus on the dynamics of the EPR effect and restoring tumor blood flow by using EPR effect enhancers. We also discuss new applications of EPR-based nanomedicine in boron neutron capture therapy and photodynamic therapy for solid tumors.

Keywords: polymer drug; EPR-effect; tumor blood flow; EPR-effect enhancers; BNCT; PDT



Citation: Islam, W.; Niidome, T.; Sawa, T. Enhanced Permeability and Retention Effect as a Ubiquitous and Epoch-Making Phenomenon for the Selective Drug Targeting of Solid Tumors. *J. Pers. Med.* **2022**, *12*, 1964. <https://doi.org/10.3390/jpm12121964>

Academic Editor: Stefano Leporatti

Received: 22 October 2022

Accepted: 24 November 2022

Published: 28 November 2022

Publisher's Note: MDPI stays neutral with regard to jurisdictional claims in published maps and institutional affiliations.



Copyright: © 2022 by the authors. Licensee MDPI, Basel, Switzerland. This article is an open access article distributed under the terms and conditions of the Creative Commons Attribution (CC BY) license (<https://creativecommons.org/licenses/by/4.0/>).

1. Introduction

The enhanced permeability and retention (EPR) effect is a property of macromolecules larger than 40 kDa or even 800 kDa (even as large as bacteria); these macromolecules include proteins such as albumin and immunoglobulin-G (IgG), polymer conjugates, liposomes, micellar drugs, nanoparticles, and other biocompatible macromolecular compounds [1–5]. The macromolecules tend to accumulate in tumor tissues much more than in normal tissues [1–5]. In 1986, Matsumura and Maeda found that the underlying mechanism of tumor-selective drug targeting is based on the unique characteristics of tumor blood vessels [6]. The causes of the EPR effect are (i) defective tumor blood vessels; (ii) various vascular effectors including nitric oxide (NO), bradykinin, vascular endothelial growth factor (VEGF), carbon monoxide (CO) produced by heme oxygenase-1 (HO-1), and prostaglandins (e.g., prostaglandin E₂, prostaglandin I₂) that facilitate extravasation; and (iii) impaired lymphatic clearance, so that macromolecular drugs remain in tumor tissues for extended periods [1,4,7–10]. The EPR effect occurs not only in primary cancers but also in metastatic cancers including lymphatic, liver, and lung metastases and in inflamed tissues [4,10–12]. Different researchers throughout the world have extensively verified the EPR effect in different tumor models as well as in cancer patients [2,13–15].

The heterogeneity of tumor tissues is another important issue because the EPR effect depends on tumor blood flow: no blood flow suggests a poor EPR effect or no EPR

effect at all [10,11,16,17]. Most experimental tumor models for evaluation of anticancer drugs utilize tumors with small diameters (about 5–7 mm) that are highly vascular and genetically homogeneous, so that the resultant positive outcomes that were expected are observed [10,11,15,16]. In contrast, cancers seen in clinical settings are highly variable—the tumor diameter, for example, can be 2–100 mm or even larger, and clinical tumors can have completely different genetic backgrounds [18–20]. Also, advanced human tumors in clinical settings have suppressed blood flow, which often results in the formation of fibrin clots or thrombi and thus unsatisfactory therapeutic effects are seen [21–23]. In addition, in tumors with a dysplastic stroma (such as pancreatic cancer), blood vessels may be weakly perfused and even collapsed or obstructed by tumor-associated fibroblasts or pericytes that adhere tightly to vascular walls, which leads to a poor EPR effect and therapeutic failure [10,24–26]. These frequent events can mislead researchers to the incorrect view of the EPR effect—that it is not fully observed in human tumors [10,11].

To overcome poor tumor blood flow and enhance delivery of drugs to tumors, our group used NO donors, so-called EPR effect enhancers, which yielded a breakthrough in our investigations [27–29]. We found that after administration of various EPR effect enhancers in combination with nanomedicines the delivery of drugs to tumors, as well as the therapeutic efficacy in advanced tumors, increased 2- to 4-fold in various tumor models [10,27–29]. These NO donors act as vasodilators to open up tumor blood vessels and increase tumor blood flow, which led to greater drug accumulation in tumors [10,27,28]. Our group also studied another type of EPR effect enhancer—CO donors—which have functions similar to those of NO donors [30–32]. CO is mainly produced in the body during heme degradation, which is catalyzed by HO-1, and has various functions including vasodilation (just like NO) and thus plays a crucial role in enhancing drug delivery to tumors [10,30,32].

This review describes the principle underlying the EPR effect, discovery of this effect, criticisms of the EPR effect, the effect's heterogeneity, and solutions for different EPR-related issues by using various chemical and physical applications. In addition, we discuss considerations related to radiation therapy, especially photodynamic therapy (PDT) and boron neutron capture therapy (BNCT), which are used for cancer treatment.

2. Discovery of the Concept of the EPR Effect

The concept of the EPR effect was first developed during an investigation of the molecular mechanism responsible for the pathogenesis of bacterial infection via activation of protease cascades involving the kallikrein system, which generates bradykinin (kinin) [33–35]. Maeda's group found that less than 1 µg of bacterial protease could induce potent extravasation or enhancement of the vascular permeability of Evans blue-bound albumin in vivo [33,34]. Maeda's group subsequently found that a similar cascade of kinin generation (e.g., prostaglandin I₂) were involved in vascular permeability in solid tumors as well as in inflamed tissues [36–38]. This finding was extremely significant because at the same time they had been working with the antitumor agent neocarzinostatin (NCS) (12 kDa) to determine how to deliver NCS to cancer tissues as well as metastatic cancers in vivo [3].

Basically, they observed the EPR effect during studies of styrene-co-maleic acid (SMA) polymer conjugated with NCS, which they named SMANCS. SMA, a synthetic polymer of 1.2 kDa, has high lipophilicity and was covalently conjugated with NCS via an amide bond [39,40]. Maeda et al. noted that when SMANCS was dissolved in lipid formulations, especially the lipid radiocontrast agent Lipiodol, and injected via a tumor-feeding artery, the tumor/blood ratio of the drug (SMANCS/Lipiodol) at 24 h after injection increased more than 2000-fold compared with the non-modified drug NCS [39–41]. Moreover, SMANCS had a longer plasma half-life, about 20 times greater than the parental drug NCS, which was rapidly washed out from blood via bile or urine [40]. At the same time, they validated this unique and important phenomenon by using plasma proteins of different molecular sizes and named it EPR effect [6,42,43]. They found that the nature of extravasation of macromolecules within a specific tumor tissue was very similar to that in inflamed

tissue that resulted from bacterial infection or inflammation and that factors affecting the inflammation of infected tissue, such as bradykinin, NO, VEGF, CO, prostaglandins, and many cytokines, were almost the same as those in cancer tissues [3,44]. Matsumura and Maeda first reported this epoch-making phenomenon in 1986 [6].

More than three decades have now passed since the discovery of the EPR effect. This effect has been verified by many researchers throughout the world who utilized various macromolecular drugs including polymer conjugates, liposomes, micellar drugs, and nanoparticles in experimental tumor models as well as in human tumors [10,16,17].

3. Criticisms and Misconceptions about the EPR Effect

Certain criticisms have been raised about the validity of the EPR effect [45,46], and some reports indicated that the EPR effect is a controversial concept in tumor drug delivery [46–49]. For example, these reports stated that nanomedicines did not produce anticancer effects at expected levels and that the EPR effect was not fully observed in clinical settings [46,47,49]. In addition, a recent report offered the opinion that nanomedicines were taken up by the transcytosis pathway and that a very small amount of drugs accumulated in the tumor via the endothelial gap [45]. Transcytosis is an active metabolic process that requires endothelial cells to rearrange their cytoskeleton and form vesicles that help to take up nanomedicines [45]. That is to say, gaps occur infrequently along tumor vessels and then nanoparticles can use active transport through trans-endothelial pathways to enter solid tumors [45]. This opinion was validated by using gold nanoparticles, with particle sizes from 15 to 100 nm, in the Zombie mouse model [45]. To validate this transcytosis-mediated tumor accumulation, however, we believe that other nanomedicines including polymer drugs, liposomes, and stable micellar drugs must be evaluated. Also, a question has arisen about this mechanism: if nanomedicines are taken up via a transcytosis process, why do nanomedicines always show greater accumulation in tumors compared with low-molecular-weight drugs? In addition, to observe the EPR effect or gaps in junctions in tumor blood vessels, permeability factors such as NO, VEGF, and bradykinin must be generated, but in the Zombie model these vascular mediators are barely found.

To address these criticisms and misunderstandings about the EPR effect and nanomedicines, we realized that certain important issues must be clarified. First, during the development of nanomedicines, the stability of the drug during circulation is quite important. For example, after intravenous injection if the active pharmaceutical ingredients, which are covalently linked to polymer conjugates, detach from the polymers or micellar drugs they become unstable in 100% blood, and as a result the nanomedicines behave as low-molecular-weight drugs and no EPR effect is observed [10,11]. Second, certain nanomedicines, especially liposomes (e.g., doxil), are quite stable, so that poor drug release into the tumor resulted and thus a less effective therapeutic outcome was noted [10,50]. Third, many nanomedicines are designed to have positive surface charges to avoid the so-called reticuloendothelial system uptake, but they quickly adhere to vascular walls because their luminal surface is negatively charged; as a result the plasma concentration decreases quite quickly after intravenous infusion [5,10]. Fourth, most tumors in clinical settings are advanced stage and large tumors with embolized blood vessels, so no or very low blood flow is seen [10,28,30]. Also, these tumors are often necrotic and demonstrate no or poor drug delivery [28].

4. The EPR Effect Is a Rational and Dynamic Phenomenon for Tumor-Selective Drug Delivery

Blood vessels in tumors are porous and do not have an architecture with fixed or rigid gaps [4,6,10]. In contrast, normal blood vessels contain tight endothelial cell-cell junctions, and cell-cell junctions can change according to microenvironmental conditions [6,10]. Maeda's group clearly showed the different architecture in tumor tissue blood vessels and normal healthy tissue blood vessels by means of scanning electron microscopy (SEM) of metastatic tumor nodules in the liver that originated from colon cancer (Figure 1) [44,51]. The blood vessels in normal tissue have clear, smooth tight junctions and no leakage of

polymeric resin (Figure 1A,B). In contrast, tumor blood vessels have irregular features, gaps between tight junctions, and polymeric resin leakage at the capillary level or in the early phase of polymeric resin leakage (Figure 1C,D) [44,51]. The gaps junctions of tumor blood vessels will open when blood pressure is elevated or after generation of various vascular mediators, followed by permeability of the tumor substratum [5,44]. Maeda's group also showed that when SMANCS/Lipiodol was infused into the tumor-feeding artery the drug was delivered selectively to tumors by the virtue of the EPR effect, and this selective delivery was clearly visualized by using computed tomography (CT) [5,29]. In addition, evidence of the EPR effect was acquired by means of radiosciintigraphy of tumors with γ -emitting gallium-67 citrate: when this agent was administered intravenously it formed a complex with transferrin (80 kDa) in the plasma that behaved as a nanomedicine. This complex accumulated selectively in solid tumors after 48–72 h and was visualized by using a γ -scintillation camera that provided clear evidence of the EPR effect [4,29].

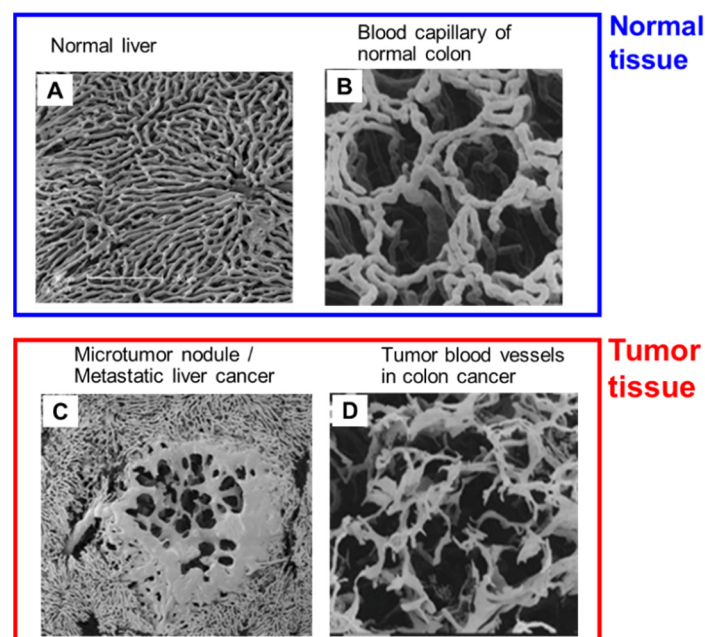


Figure 1. Comparison, via scanning electron microscopy (SEM), of a normal tissue blood vessel (A,B) and a tumor blood vessel (C,D) obtained from metastatic tumor nodules in the liver that originated from colon cancer. Blood vessels in normal liver (A) and healthy colon (B) show clear, smooth tight endothelial gaps and no leakage of polymeric resin. In contrast, tumor vessels, both in liver metastasis (C) and in colon cancer (D), show leaky blood vessels with irregular features. These SEM images were taken and modified from ref. [44].

In addition to Maeda's group, many research groups throughout the world validated the existence of the EPR effect [15,24,52,53]. Lee et al. recently provided strong evidence for the EPR effect and quantified the effect in human breast tumors including metastatic tumors [13]. They evaluated the EPR effect in 19 patients with HER2-positive metastatic breast cancer by using the ^{64}Cu -labeled nanoparticle ^{64}Cu -MM-302 (^{64}Cu -labeled HER2-targeted PEGylated liposomal doxorubicin) and by imaging via positron emission tomography and CT [13]. They found significant drug accumulation in tumors as a consequence of the EPR effect after 24–48 h of drug treatment in the patients [13]. Ding et al. also analyzed the EPR effect in human renal tumors via X-ray computed tomography and correlated this effect in human tumors with that in animal models [14]. As a surprising result, they found that a considerable EPR effect was present in human renal tumors: more than 87% of human renal tumors showed the EPR effect, with significant diversity and heterogeneity in different patients. All the evidence cited above strongly indicates that the EPR effect is a rational and universal mechanism for tumor-selective accumulation of nanomedicines.

5. Heterogeneity of the EPR Effect: An Obstacle to Successful Nanomedicine Therapy in Clinical Settings

The heterogeneity of the EPR effect, or embolization of tumor blood vessels, is one issue that mislead researchers about nanomedicines as well as the EPR effect [11,28]. In general, experimental mouse tumors are different from clinical tumors: mouse tumors are smaller (3–10 mm in diameter) and have sufficient tumor blood flow and less or no heterogeneity, so that adequate drug delivery to tumors occurs, based on the EPR effect, and excellent antitumor effects are seen [10,11,28]. In contrast, tumor in clinical settings can be 2–100 mm in diameters or even larger, and these tumors are genetically highly variable or have considerable heterogeneity [11,44]. Also, these late stage tumors have many necrotic areas or occluded blood vessels and no typical physiological blood flow (Figure 2A) [28,44]. We recently determined that the coagulation or thrombogenic system in tumor tissue was highly expressed as tumors grew [37], which resulted in occlusion or embolization of tumor blood vessels and consequently a poor EPR effect, thus reducing the success of cancer chemotherapy in clinic. In this regard, tissue factor (TF) involving the coagulation cascade and chemotactic factors may be involved in obstructing drug delivery based on the EPR effect [10]. Navi et al. recently reported that cancer patients have an increased risk of arterial thromboembolism; however, when this excess risk begins is not clear [21,22]. They studied 374,331 patients 67 years old or older with a new primary diagnosis of breast, lung, prostate, colorectal, bladder, uterine, pancreatic, or gastric cancer or non-Hodgkin lymphoma from 2005 to 2013 and compared the risks of arterial thromboembolic events of cancer groups and no-cancer groups during 30-day periods in the 360 days before the date of cancer diagnosis [21,22]. They found no differences in arterial thromboembolic events from 360 to 151 days before cancer diagnosis between the two populations, but from 150 to 1 day before cancer diagnosis, the risks of arterial thromboembolic events were much higher in cancer patients compared with matched controls [21]. These findings suggest that the nature of tumors in clinical settings is not similar to that of experimental mouse tumors, so additional enhancement of tumor drug delivery is required by restoring tumor blood flow. Figure 2B illustrates the method of tumor blood flow restoration.

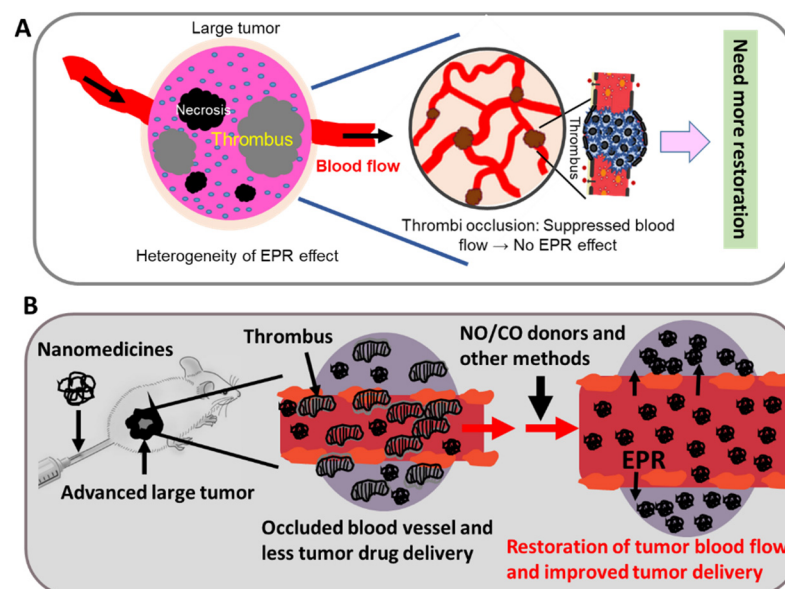


Figure 2. Illustration of an embolized blood vessel in an advanced tumor (A) and the strategy used to overcome the suppressed blood flow (B). Late-stage tumors possess many necrotic areas, and a fibrin clot resulted in thrombus formation, which blocked tumor blood flow (A). In this case no typical enhanced permeability and retention (EPR) effect existed, and additional enhancement of tumor blood flow was needed. (B) Mechanism of tumor blood flow restoration by using different methods or EPR effect enhancers.

6. NO Donor-Induced Enhancement of Drug Delivery to Tumors as Well as of Therapeutic Effects

Our group has made great progress in overcoming embolized blood vessels by using NO donors [27,28]. We studied the NO donors nitroglycerin (NG), L-arginine (L-Arg), hydroxyurea (HU), and isosorbide dinitrate (ISDN). Among these agents, NG has been used as a medication for angina pectoris for more than century [54]. NG is administered as an ointment or orally, which selectively generates NO in cardiac infarct tissue and in cancer tissue that is hypoxic and has slightly acidic pH [54,55]. NG first produces nitrite and then converts it to NO by means of nitrite reductase; NO acts as a vasodilator to open up blood vessels [7,56,57].

L-Arg is the substrate of nitric oxide synthase (NOS), especially the inducible form of NOS (iNOS), which is highly expressed in most tumors and inflamed tissues, more than in normal cells [58,59]. iNOS is derived from infiltrated macrophages that produce NO in tumors with relatively high specificity [28,50,58].

HU is used to treat cancer of white blood cells called chronic myeloid leukemia, sickle-cell anemia, cervical cancer, and polycythemia vera. Our group found that HU, like other NO donors, generated NO and increased tumor blood flow [28]. Gladwin et al. and Sato et al. reported [60,61] that, as a possible mechanism, HU generated NO via NOS, because HU is the intermediate in production of NO from L-Arg, and HU may thus demonstrate tumor-selective NO production [10,28,29,60,61].

ISDN is used to treat heart failure and spasms and to treat and prevent chest pain from inadequate blood flow to the heart [62,63]. The molecular mechanism of ISDN is similar to that of other nitrites and organic nitrates: ISDN is converted to NO through an active intermediate compound that activates the enzyme guanylate cyclase [62]. This activation induces the synthesis of cyclic guanosine 3',5'-monophosphate, which then activates a series of protein kinase-dependent phosphorylation processes in smooth muscle cells, and thus vasodilation occurs [10,29,62,63].

We used combination therapy with different nanomedicines to study the four above-described NO donors in various mouse and rat tumor models. NG was applied as an ointment at the dose of 0.1 mg/mouse [28]. L-Arg at 50 mg/mouse, HU at 50 mg/kg, and ISDN at 30 mg/kg were administered intraperitoneally immediately after drug injection [10,28,29]. To evaluate the enhancement of drug delivery to tumors by these NO donors, i.e., the EPR effect enhancers, we used various tumor models to test five nanomedicines developed by our group: P-THP—*N*-(2-hydroxypropyl)methacrylamide (HPMA) copolymer conjugated with pirarubicin [64]; P-PyF—HPMA polymer-conjugated pyropheophorbide [65]; PZP—HPMA polymer-conjugated zinc protoporphyrin (ZnPP) [66]; SMA-CDDP—the micellar drug cisplatin ion complex with SMA polymer [67]; and SGB-complex—the complex formed with SMA copolymer conjugated with glucosamine and boric acid (BA) [68]. We first investigated the enhancement of drug delivery in mouse sarcoma S180 and colon carcinoma C26 tumor with different EPR effect enhancers and found that tumor drug accumulation increased 2- to 3-fold compared with the nanomedicine alone treatment group, as determined by means of fluorescence spectroscopy and IVIS imaging (the *in vivo* fluorescence imaging system) (Figure 3A,B) [28,29]. As an interesting result, drug accumulation in normal tissues did not increase significantly after combination treatment with NO donors (Figure 3A) [28]. To support our hypothesis, we measured tumor blood flow with and without various NO donors and found that tumor blood flow increased 2- to 3-fold when combination treatment with NO donors was used (Figure 3C) [28]. We also investigated the therapeutic effects of NO donors in S180, C26, and B16 melanoma tumor models; we found a 2- to 4-fold enhanced antitumor effect with different NO donors (Figure 3D) [28,29]. In addition, we studied the improved therapeutic effects after use of azoxymethane (AOM), which induced autochthonous colon tumors in mice, and dimethylbenzene[*a*]anthracene (DMBA), which induced breast tumors in rats [28]. To produce colon tumors, AOM at 10 mg/kg (0.3 mL/mouse) was injected intraperitoneally into ICR mice, and 1-week later mice were fed 2% dextran sodium sulfate (DSS) in drinking water for

7 days. After 8–10 weeks of AOM administration, mice developed colon tumors [28]. The DMBA-induced breast tumor model was established by administering DMBA: 10 mg of DMBA was dissolved in 1 mL of corn oil and was given orally to SD rats; breast tumors were observed 12–14 weeks after DMBA administration [28]. In both chemically induced tumor models, we also found that combination treatment with nanomedicines and EPR effect enhancers increased the therapeutic effect 2- to 3-fold (Figure 4) [28]. We utilized chemically induced tumor models because these tumors can grow spontaneously and are similar to clinical tumors [10,28].

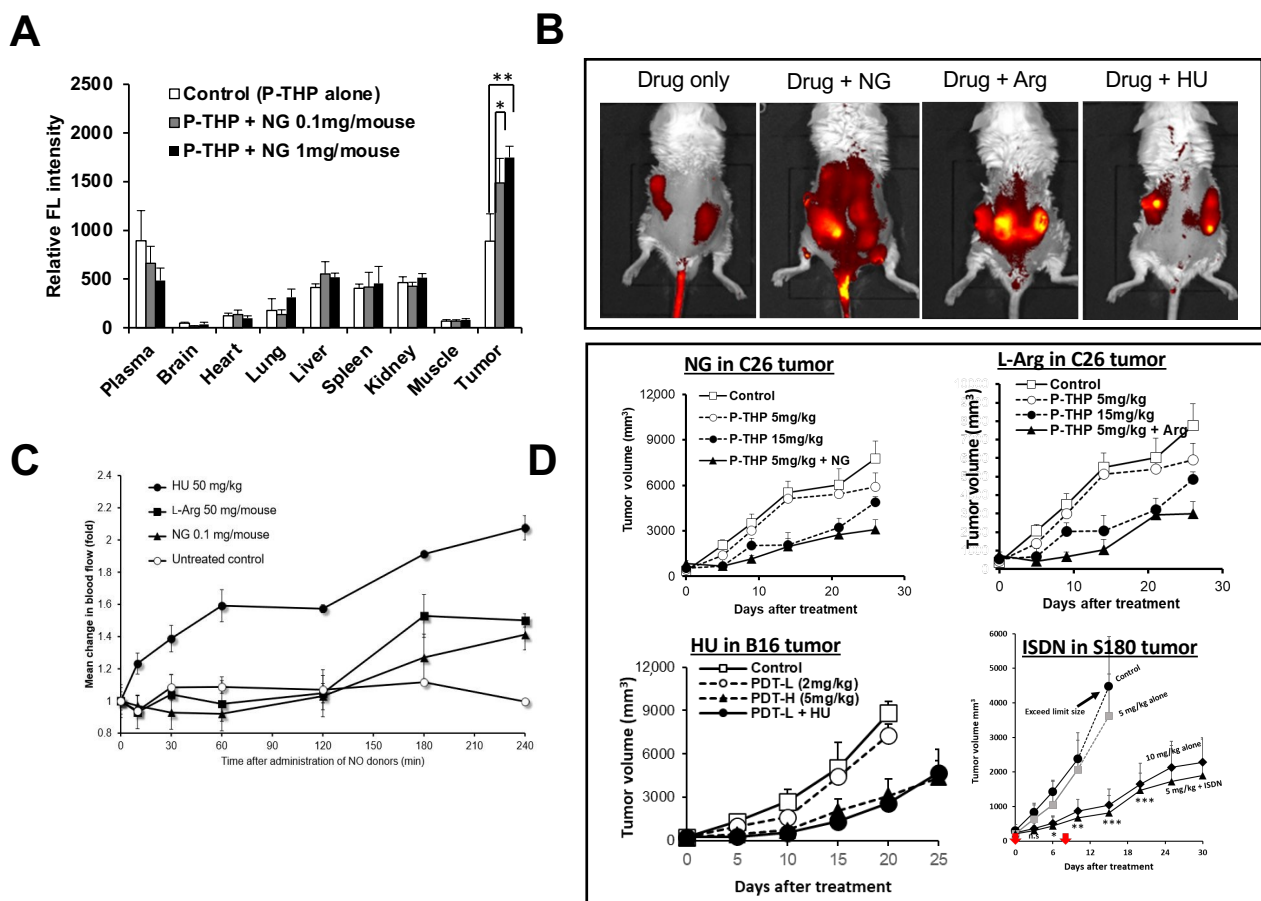


Figure 3. Enhancement of tumor drug accumulation and therapeutic efficacy by using different nitric oxide (NO) donors in implanted tumor models. We first investigated increased drug delivery in various solid tumors that had been generated via subcutaneous administration of cancer cells (2×10^7 cell/mL, 100 μ L/mouse) on the dorsal skin. When tumor diameters measured 10–12 mm, the polymer drug was administered intravenously (iv) in combination with NO donors, e.g., nitroglycerin (NG) at the dose of 0.1–1 mg/mouse as an ointment, L-arginine (L-Arg) at 50 mg/mouse intraperitoneally (ip), hydroxyurea (HU) at 50 mg/kg ip, and isosorbide dinitrate (ISDN) at 30 mg/kg, ip. After 24 h of drug treatment, drug accumulation was measured in tumor tissue homogenate by means of fluorescence spectroscopy (A) and in vivo imaging by IVIS (IVIS XR; Caliper Life Sciences) (B). The improved blood flow in S180 tumors with different NO donors was measured by using a laser Doppler flowmeter (ALF21: Advance Co., Ltd.) (C). (D) Enhancement of the antitumor effect of various nanomedicines including P-THP [*N*-(2-hydroxypropyl) methacrylamide (HPMA) copolymer conjugated with pirarubicin], PZP [HPMA polymer-conjugated zinc protoporphyrin (ZnPP)], P-PyF (PHPMA polymer-conjugated pyropheophorbide), and SGB-complex [complex formed with styrene-co-maleic acid (SMA) copolymer conjugated with glucosamine and boric acid (BA)] with EPR effect enhancers in different tumor models. Red arrows indicate the (iv) injection point. PDT indicates photodynamic therapy with PZP, L: low dose, H: high dose. Data are expressed as means \pm SD. $n = 5$, * $p < 0.05$, ** $p < 0.01$, *** $p < 0.001$. For details, please see Islam et al. [28,29].

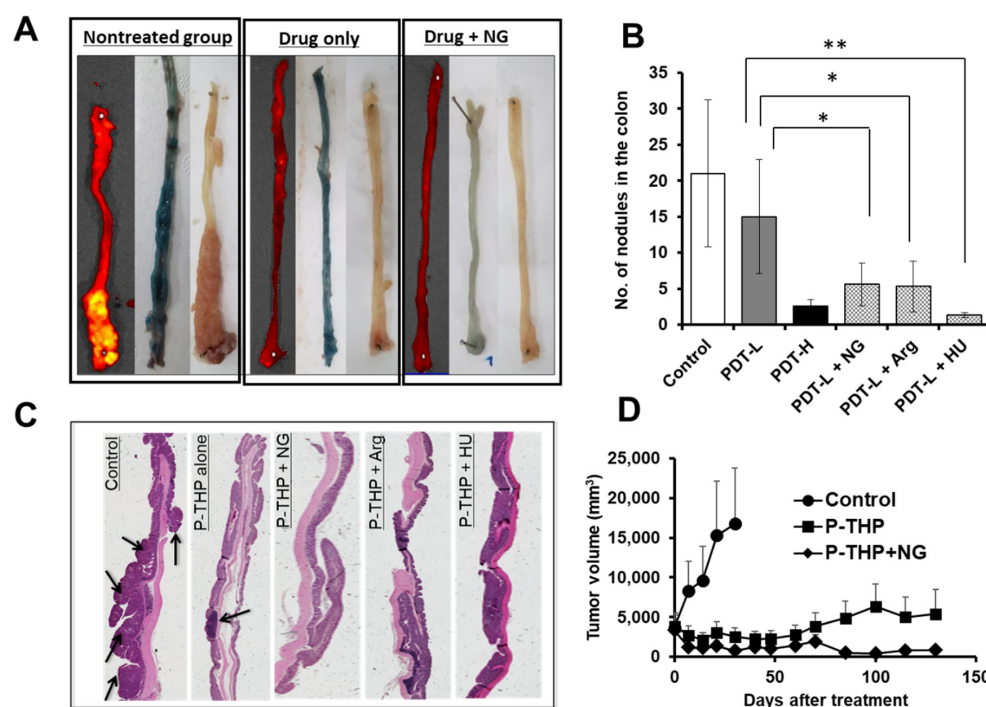


Figure 4. Improvements in therapeutic effects of nanomedicines by using NO donors in chemically induced tumors. Autochthonous colon tumor was developed by administering the chemical azoxymethane (AOM, 10 mg/kg, intraperitoneally) followed by 1 week of drinking 2% dextran sodium sulfate (DSS). At 8–10 weeks after AOM injection, tumor nodules that appeared in the colon were confirmed by examining 2 or 3 randomly killed mice. P-THP at 15 mg/kg iv was infused with NG, and tumor nodules in the colon were visualized by using bovine serum albumin conjugated with rhodamine or Evans blue after 30–40 days of P-THP treatment (A). Another nanomedicine, PZP, which was used with light irradiation (PDT) and EPR effect enhancers, produced a similarly improved therapeutic effect (B). Enhancement of the anti-cancer effect with NO donors in colon tumors was confirmed by means of macroscopic and microscopic histology (C). Arrows indicate tumor nodules in the colon. (D) Enhanced therapeutic effect of P-THP with an NO donor in an advanced breast tumor in the rat. Breast tumors were generated by using dimethylbenz[*a*]anthracene (DMBA, 10 mg/mouse, orally), and tumors appeared 12–14 weeks after DMBA administration. Data are expressed as means \pm SD. $n = 5$, * $p < 0.05$, ** $p < 0.01$. For details please see Islam et al. [28].

7. Enhancement of the Anticancer Effects of Drugs by Using CO Donors

Our group also developed another method to enhance drug delivery to tumors by using CO donors [30]. CO is a gaseous molecule that is primarily generated in the body during heme degradation, is catalyzed by HO, and has vasodilation functions that are similar to those of NO [30,32]. The inducible form of HO (HO-1) is expressed at high levels in tumors; also called heat shock protein 32, it has antiapoptotic and antioxidant activities and thus facilitates tumor cell growth and survival [10,30,69]. However, detailed mechanisms of vasoregulation induced by CO are not clearly understood.

Our group developed two nano-sized CO donors: SMA/CORM2 micelles and polyethylene glycol (PEG)-conjugated hemin (PEG-hemin) [31,70]. The reasons for choosing nano-donors are the slow CO release and the tumor-selective accumulation based on the EPR effect [10,32,70]. Of these donors, SMA/CORM2 is an extrinsic supplier of CO and can supply CO slowly because of its nano size [10,30]. The other donor, PEG-hemin, induces HO-1 [31]. Usually, the HO-1-inducing agent hemin is barely soluble in water and has a short plasma half-life and comparatively less accumulation in tumors [30,31]. However, the nano formulation has an improved plasma half-life and drug delivery to tumors [30,31]. Our group showed that both CO donors produced CO more selectively in tumor tissues than in normal tissues, which increased tumor drug delivery 2- to 3-fold by restoring tu-

mor blood flow, as evaluated by fluorescence angiography and fluorescence imaging IVIS (Figure 5) [30]. In addition, when various nanomedicines (e.g., P-PyF) were administered together with these nano-CO donors, the anticancer effect improved 2- to 3-fold in different solid tumor mouse models [30]. These data suggest that CO donors have functions similar to those of NO donors.

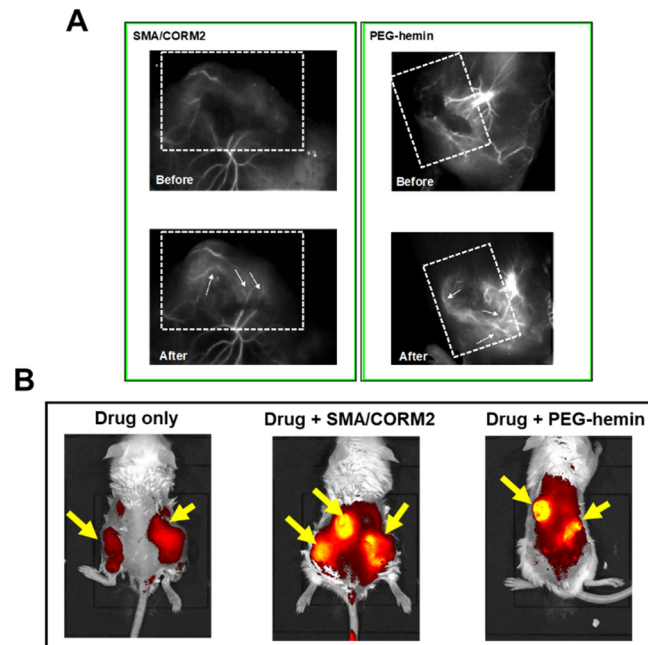


Figure 5. Enhancement of the EPR effect via nano-sized carbon monoxide (CO) donors [SMA/CORM2 and polyethylene glycol (PEG)-hemin] in S180 and C26 tumors. Fluorescence angiography demonstrated improved tumor blood flow after use of SMA/CORM2 and PEG-hemin in S180 tumor-bearing mice (A). Increased tumor delivery of P-PyF given at 5 mg/kg iv in the C26 tumor model with CO donors was confirmed by means of in vivo fluorescence imaging (IVIS) at 24 h after drug injection (B). Arrows indicate the tumor. Please see Fang et al. [10,30].

8. Other EPR Effect Enhancers Used to Improve Drug Delivery to Tumors

To enhance tumor drug delivery, various chemical and physical methods, in addition to NO and CO donors, have been developed [10]. These chemical methods include utilizing tumor necrosis factor α (TNF- α), anti-tissue factor and antibody drug conjugate (anti-TF-ADC), recombinant, micellar forms of tissue plasminogen activator (tPA), anti-VEGF receptor 2 (VEGFR2) antibody, (DC101), Angiotensin II receptor blockers (ARBs), cilengitide, and so on. Physical techniques consist of radiation therapy, sonoporation or ultrasound (US) with microbubbles (MBs), hyperthermia (HT), and PDT. These methods of drug delivery are described below.

TNF- α is a pleiotropic pro-inflammatory cytokine with vascular permeabilizing activity [71]. For example, it is applied during isolated limb perfusion to enhance delivery of chemotherapeutic drugs to tumor tissue [71,72]. Seki et al. showed that TNF- α enhanced endothelial cell permeability and increased drug delivery 2- to 3-fold in the EL4 tumor model and in mice with cerebral brain metastases [71].

Pancreatic cancer is rarely diagnosed at early stages because it often does not cause symptoms until after it has spread to other organs [73]. Despite recent advancements in pancreatic cancer treatment, patients with this cancer have only an 8% chance of 5-year survival [74]. Overexpression of tissue factor (TF) has been seen not only in tumor cells but also in tumor stromal cells, so a cure of pancreatic cancer is not easy [74]. Matsumura's group reported that anti-TF-ADC, compared with control ADC treatment, significantly enhanced drug accumulation and penetration of tumors in a stromal-rich orthotopic pancreatic cancer model [74,75].

The blood vessels in early-stage tumors are homogeneous, and blood flow is relatively high [22]. In contrast, blood vessels in advanced late-stage tumor tissues in clinical settings are frequently embolized or occluded by fibrin clots, and thus tumor tissues become necrotic, with limited blood flow, and hypoxic [10,68]. The use of thrombolytic agents such as tPA in combination with other nanomedicines or drug carriers may lead to enhanced therapeutic effects by increasing drug delivery close to the solid tumor via fibrin degradation and blood flow restoration [76,77]. Nagasaki's group reported that administration of tPA together with nanomedicines resulted in 2- to 3-fold-enhanced tumor drug delivery as well as therapeutic efficacy in the A549 tumor xenograft tumor model [76,77].

VEGFR2 is a Kinase insert domain receptor (KDR, a type IV receptor tyrosine kinase). The concept of anti-VEGFR2 was established by developing a monoclonal rat anti-mouse VEGFR2 antibody (DC101) and showing that it potently blocked the binding of VEGF to its receptor, inhibited VEGF-induced signaling, and strongly blocked tumor growth in mice through an anti-angiogenic mechanism [78]. Anti-angiogenic drugs are initially designed for oxygen- and nutrient-deprivation in tumor tissues, however, these agents showed limited therapeutic outcome in clinical setting [79]. Therefore, a strategy to use angiogenesis inhibitors as a tumor blood flow modulator to increase the delivery efficiency of nanoparticles has been developed [80]. In this strategy, an intermediate dose of an anti-VEGF receptor 2 (VEGFR2) antibody, DC101, was applied and successfully normalized tumor vessels to a certain extent such that oriented vascular structure was achieved with increased blood perfusion, decreased vascular density, and reduced necrotic and hypoxic regions [81]. As a possible mechanism Vikash et al. mentioned that, DC101 normalized disorganized tumor vessels by pruning immature vessels and reinforcing the remaining vasculature as well as decreased interstitial fluid pressure (IFP), thus leading to a more uniform and enhanced delivery of a model protein [82]. Coadministration of DC101 with Doxil (~125 nm in size) or Abraxane® (~12 nm in size after dilution in plasma) showed about 3-fold enhancement of tumor drug delivery in breast tumor model [80].

Angiotensin receptor blockers (ARBs), also known as angiotensin II receptor antagonists, are used to treat high blood pressure and heart failure. ARBs can be used to enhance EPR based tumor drug delivery because they amplify the effect of substances like bradykinin, which promote vessel permeability and dilation through the loosening of the fasciae adherens, i.e., the endothelial cadherin mediated intercellular connections [17]. ARBs also modulate the expression of extracellular matrix (ECM) components (e.g., reduction in collagen expression), which leads to vessel decompression and to enhanced EPR effect [83,84]. Various ARBs, for example losartan, which is clinically used to treat chronic kidney diseases and hypertension, but also showed promising preclinical results in cancer treatments, can be used for this purpose [85]. Jain and colleagues showed the combination treatment of losartan significantly improved tumor drug delivery in E0771 and 4 T1 breast carcinoma as well as AK4.4 and Pan-02 pancreatic carcinoma tumor model [85]. A preliminary data indicate that the losartan-based combination therapy led to a decrease in tumor size and in some cases even enabled surgical resection [2]. For example losartan based combination therapy in phase II study showed 2-year overall survival exceeded 60%, and the number of patients where a resection of the tumor was possible after combination therapy exceeded 50%, resulting in 2-year survival in the resected patient population of close to 80% [2].

Wong et al. proposed a strategy named vessel promotion, which focusses on increasing angiogenesis resulting in more vessels and eventually a higher delivery of chemotherapeutic [86]. Cilengitide, a cyclic peptide, which binds to $\alpha v \beta 3$ integrins and is usually associated with anti-angiogenesis [87]. This vessel promoting agent was treated in combination with verapamil, a calcium channel blocking agent leading to higher blood flow, resulting in a significant increase of blood vessel perfusion of 10% [2]. The cotreatment of cilengitide, verapamil and gemcitabine, showed a significantly increased mean survival time, approximately doubled compared to gemcitabine only group in a mutagenic mouse model of pancreatic cancer (KPC mice) [2].

Radiation therapy, a quite common cancer treatment, is routinely used in approximately half of all patients with solid tumors [88]. Besides inducing direct antitumor effects, radiotherapy can play an important role in enhancing drug delivery to tumors—both penetration of drugs and their accumulation in tumors [88,89]. Radiation can be used as a physical method to enhance tumor drug delivery: it activated targeted endothelial nanomedicines to induce physical vascular damage related to increased photoelectric interactions [88]. Radiation applied in combination with nanomedicines produced about a 2-fold increase in tumor drug delivery in a human pancreatic tumor model (h-PDAC) and in R3230 mammary adenocarcinomas [88,89].

HT is another physical modality utilized to improve drug delivery to tumors. This treatment relies on local heating of tumors to temperatures up until ~70 °C, and it can be administered in the form of microwaves, radiofrequency radiation, and US [90–92]. Mild HT in the range of 39–42 °C promotes perfusion, vasodilation, and vascular permeability, and it enhanced tumor drug delivery, about 2-fold in SK-VO-3 ovarian carcinoma and in the DU145 prostate cancer model [88,92].

Sonoporation can be defined as the permeabilization of cell membranes induced by rapid expansion and compression of MBs after exposure to US [93]. With low-intensity US, MBs disrupted the endothelium and resulted in significantly enhanced tumor drug accumulation in various tumor models [10,88]. That is, when US with MBs was applied with nanomedicines the drug delivery to tumors significantly improved in the highly cellular A431 epidermoid xenografts, the highly stromal BxPC-3 pancreatic carcinoma xenograft model, and clinical pancreatic cancer [10,88,93].

PDT is popular for treating acne and is widely utilized in medicine. We provide details about its application in cancer treatment later in this article. PDT is also applied to enhance tumor drug delivery [94]. Li et al. reported that PDT destroyed tumor-associated fibroblasts and enhanced therapeutic efficacy about 18- to 20-fold in bilateral 4T1, U87MG, MDA-MB-435S, and PC-3 tumor xenograft models [94,95].

All the findings described above suggest that enhancement of tumor drug delivery is quite important. Table 1 summarizes currently used EPR effect enhancers.

Table 1. EPR effect enhancers used to improve drug accumulation in tumors and their modes of action.

Methods	Drugs/Agents	Tumor Model	Outcome (Augmentation)	Brief Mechanisms
Vascular mediators	NO generating (i) NG (ii) L-Arg (ii) HU (iv) ISDN (v) Sildenafil	Xenograft tumor S180, C26, B16, 4T1 Chemically induced AOM/DSS-induced colon tumor and DMBA-induced breast tumor	2- to 5-fold	Open tumor blood vessels as a vasodilator and thus improve drug delivery to tumors [10,27–30,96]
	CO generating (i) SMA/CORM2 (ii) PEG-hemin	S180, C26, B16	2- to 3-fold	Functions similar to those of NO donors [10,30]
	Others (i) Tumor necrosis factor- α (TNF- α) (ii) Anti-tissue factor-antibody drug conjugate (anti-TF-ADC) (iii) Tissue plasminogen activator (tPA) (iv) anti-VEGF receptor 2 (v) Angiotensin II receptor blockers	(i) EL4 (ii) Pancreatic cancer (iii) A549 (iv) Breast tumor (v) 4T1, AK4.4, E0771, Pan-02	(i) 2- to 3-fold (ii) Significantly (iii) 2- to 3-fold (iv) 3-fold (v) Significantly	(i) Increase endothelial cell permeability [71] (ii) Enhance penetration capacity [74] (iii) Restore blood flow via fibrinolysis [76] (iv) Normalized disorganized tumor vessels by pruning immature vessels [78–82] (v) promote vessel permeability and dilation through the loosening of the fasciae adherents [2,79–85]

Table 1. Cont.

Methods	Drugs/Agents	Tumor Model	Outcome (Augmentation)	Brief Mechanisms
Physical methods	(i) Radiation therapy	(i) h-PDAC, R3230	(i) 2-fold	(i) Induce physical vascular damage related to photoelectric interaction [80,88]
	(ii) Hyperthermia	(ii) SK-VO-3, DU145	(ii) 2-fold	(ii) Improve perfusion, vasodilation, and vascular permeability [80,88]
	(iii) Ultrasound (US) with microbubbles (MBs)	(iii) A431, BxPC-3	(iii) Significantly	(iii) Disrupt endothelium [80,88]
	(iv) PDT	(iv) 4T1, U87MG, MDA-MB-435S, and PC-3	(iv) 18- to 20-fold	(iv) Damage tumor associated fibroblasts [80,88]

9. Limitation of Using EPR Effect Enhancers

Although, the EPR effect enhancers improve the tumor drug delivery as well as therapeutic efficacy, but there are some limitations of using EPR-enhancing agents. The risk factor can be divided into two categories: systemic adverse reactions based on their pharmacological effects and effects on the tumor due to altering the tumor environment [80]. The major drawback of vasodilators is hypotension [97], and the vasodilator effect as an EPR enhancer should be transient. In addition, NO or CO is a gaseous molecule and they have various bioactivities, both good and bad [10,98]. Under this situation, cautions must be noted because they may cause unexpected side effects when combined with anticancer drugs [80]. NO also plays a role in tumorigenesis, for example, tumor-cell-derived NO promotes tumor progression by induction of tumor-cell invasion, proliferation and the expression of angiogenic factors [99]. The inducible isoform of NOS (iNOS), which generates high concentrations of NO, mediates neoplastic transformation in oncogene- and chemical-induced tumorigenesis models, however conflicting opinion are reported in the literature [98,99].

Angiogenesis inhibitors exhibit some adverse effects on their own such as elevation of blood pressure [100]. However, some reports showed that anti-angiogenic drugs can normalize disorganized tumor vasculature only at the intermediate dose, yet a high-dose can induce the closure of endothelial fenestration and pruned vessels, which leads to a reduction of tumor blood perfusion and thwarts the delivery of anticancer drugs [80,81].

Bharadwaj et al. reported [101] that fibrinolytics agents may increase the chance of cancer metastasis and facilitate the tumor growth. Moreover, systemically administered fibrinolytic agents may cause intracranial hemorrhage, intracranial neoplasm or trauma, hypertension, history of ischemic stroke, and so on [80,102].

Above all results suggest that EPR effect enhancers are involved in several risk, so we need to normalize using enhancers as a combination therapy. Moreover, tumor selective delivery of EPR-enhancer is another important issue need to be clarified, maybe nano formulation of EPR enhancing agent is one possible way for tumor selective accumulation.

10. EPR-Based Nanomedicine Breakthrough in BNCT Used in Cancer Treatment

BNCT is a cell-selective radiation technique that depends on α -rays emitted from boron-10 (^{10}B) atoms when neutrons hit the atoms [103,104]. When boron delivery agents enter tumor tissues and enrich tumor cells, the thermal neutrons trigger fission of boron atoms, which leads to release of ^{10}B atoms and then release of α particles (^4He) and recoil lithium particles (^7Li) [104,105]. The released α particles are toxic for cells and can result in cell destruction, bouncing out up to 10 μm , which is almost the size of the cells; for this reason this technique is called cell-selective radiation therapy [106]. The first clinical use of sodium borocaptate (BSH) for BNCT was reported by the Japanese scientist Hiroshi Hatanaka in 1960; boronophenylalanine (BPA) was introduced for clinical use by another Japanese scientist Y. Mishima in 1988–1989 [107]. Clinical trials of BNCT for treatment of glioblastoma multiforme and/or melanoma and, more recently, head and neck tumors and liver metastases, with BPA or BSH as the ^{10}B carrier, have been performed in many

countries including Argentina, Europe, Japan, Taiwan, and the United States [96,103]. Thus, BNCT is not a modern concept, although clinical progress with this method has been quite slow, probably because of the lack of tumor-selective drug accumulation and terrible adverse effects [16,103,108]. Conventional borono-drugs, which are commonly used in clinical settings, are low-molecular-weight drugs that are distributed indiscriminately throughout the body, particularly in the skin, when given intravenously [16,68]. As a result, when neutrons are used to irradiate the whole body these low-molecular-weight drugs produce adverse effects such as skin damage and mucositis, among others [96,103]. Macromolecular drugs, however, have the advantage of tumor-selective accumulation because of the EPR effect [6]. Figure 6A illustrates the problems with conventional BNCT and strategies for successful BNCT. Our group had a breakthrough in our studies to address the clinical drawbacks related to BNCT: we developed a novel multifunctional polymer conjugate drug—the SGB-complex [68]. This SGB-complex formed spontaneous micelle, manifested a single peak by gel permeation chromatography, and had a diameter of 10–15 nm by transmission electron microscopy and dynamic light scattering [68]. We found that intravenously injected SGB-complex bound with albumin during circulation and had a plasma half-life of 8 h in mice; it accumulated in tumor tissues about 10 times more than in normal tissues [68,109]. We developed the SGB-complex primarily for BNCT, but surprisingly we found that it can inhibit cancer cell growth effectively under mildly hypoxic conditions (pO_2 , 6–8%), which resemble tumor microenvironments [48,68]. In addition, the SGB-complex significantly suppressed tumor growth in various mouse tumor models (e.g., mouse sarcoma S180 and colon carcinoma C26) even without neutron irradiation [68]. We hypothesized that, as a possible mechanism, the SGB-complex inhibited glycolysis in cancer cells and affected mitochondrial functions [68,108]. We noted that the SGB-complex released free BA in tumor tissue (pH 5.5–6.5); liberated BA may compete with phosphate in the phosphorylation of glucose to glucose 1-phosphate and may thus inhibit glycolysis in cancer cells [29,68,110]. According to the Warburg effect, under hypoxic conditions cancer cells depend predominantly on energy production via glycolysis instead of the tricarboxylic acid cycle [111]. Thus, suppression of glycolysis in cancer cells will lead to cell death. To confirm our hypothesis, we measured glucose uptake, lactic acid production in hypoxia-adapted HeLa cells, and tumor tissue pH *in vivo* and found that the SGB-complex significantly inhibited glucose uptake and lactic acid secretion in HeLa cells [68]. Moreover, tumor pH after intravenous injection of the SGB-complex shifted from slightly acidic to neutral, which indicates inhibition of lactic acid production [68]. All the data presented above provide consistent evidence that the SGB-complex inhibited glycolysis in cancer cells. Our data suggest that the SGB-complex is more sensitive in hypoxic conditions than normoxic condition, which means that this nanomedicine is ideal for advanced late-stage cancers, which have low pO_2 , in clinical settings.

We also confirmed excellent anticancer effects of the SGB-complex after neutron irradiation *in vitro* and *in vivo*. We used human oral squamous carcinoma cells *in vitro* and we found, surprisingly, that the cells treated with the SGB-complex at 8 $\mu\text{g}/\text{mL}$ (BA equivalent) demonstrated about 16-fold greater cytotoxicity after 10 Gy neutron irradiation when compared with the group treated with the same dose of neutron irradiation alone (no drug) [68]. We also investigated the antitumor effect of the SGB-complex after neutron bombardment in C3H mice bearing human oral squamous cells carcinoma (SCC VII), and we found that the SGB-complex at 10 mg/kg significantly suppressed tumor growth at days 14 and 21 after a single neutron irradiation dose compared with irradiation alone ($6 \times 10^8 \text{ n}/\text{cm}^2/\text{s}$ for 30 min) or compared with the SGB-complex alone treatment group [68,108]. One hallmark result we observed that neutron irradiation of SGB-complex-treated mice did not affect the skin of the mice, nor were other common toxic effects of BNCT treatment (e.g., mucositis, systemic toxicity) [16,68,108]. These common phenomena were seen in treatment with BPA + neutron irradiation or other conventional borono-drugs [16,29,68,103,108]. These results indicate the promising future of the SGB-complex for BNCT in clinical settings. Figure 6B illustrates the multiple modes of action of the SGB-complex.

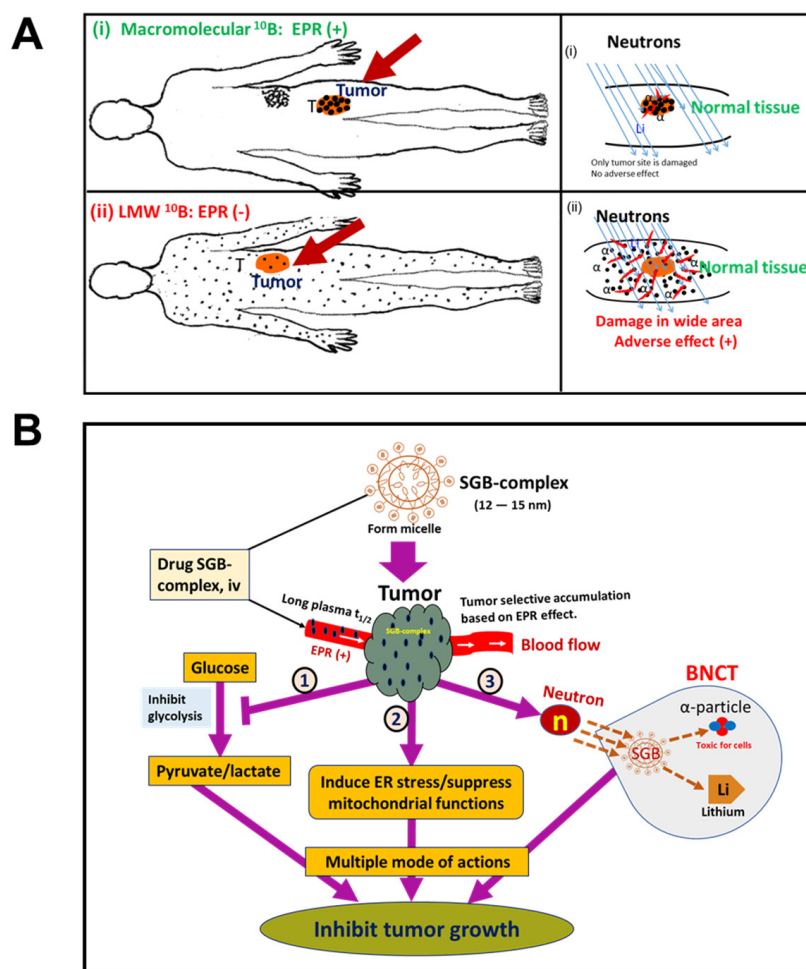


Figure 6. The strategy for successful boron neutron capture therapy (BNCT) (A) and multiple modes of actions of the SGB-complex (B). The upper panel of (A) (i) shows tumor-selective accumulation of a macromolecular borono-drug and α particles only at the tumor site. The lower panel (ii) shows that low-molecular-weight (LMW) drugs are distributed throughout the whole body and produce severe side effects. (B) Multiple mechanisms of tumor cell killing by the SGB-complex, which our group developed. ER, endoplasmic reticulum. Please see Islam et al. [70]. The image of (A) was taken from the ref. [16] and (B) was modified from ref. [68].

11. The Significant Role of EPR-Based Nanomedicine in PDT

PDT has been known for more than 100 years, but its practical impact in cancer treatment has been negligible [11,112]. PDT is a treatment that utilizes a photosensitizer (PS) followed by light irradiation. When a PS is irradiated by absorbing light at certain wavelengths, the energy level of the PS increases, a photoactivation reaction occurs that causes fluorescence emission and formation of singlet oxygen ($^1\text{O}_2$) from molecular oxygen (O_2), and the energy level of the PS will fall to the ground state [11,113]. $^1\text{O}_2$ is a reactive oxygen that plays a role as an oxidative reagent in cells and can lead to cell killing or mutation by damaging nucleic acids, proteins, and lipids [11,112,113]. Commonly used PSs in clinical settings are Photofrin[®], temoporfin (Foscan[®]), motexafin lutetium, palladium-bacteriopheophorbide, tri ethyl etiopurpurin (Purlytin[®]), verteporfin (Visudyne[®]), talaporfin (Laserphyrin[®]), and some modified versions of PSs [114]. All are low-molecular-weight compounds, which do not manifest the EPR effect, and thus they are distributed throughout the entire body, especially the skin [11,65]. When light is irradiated, $^1\text{O}_2$ generation occurs wherever the excitation light is accessible in the presence of a PS, and thus a hypersensitivity reaction of the skin is observed [10,11]. However, nano-PSs can solve this problem, because of the tumor-selective accumulation of drug by virtue of the EPR effect [10,11,66].

Maeda’s group developed several nano-PSs including PZP [66], P-PyF [65], PEG-ZnPP [115], SMA-ZnPP [116], and others. They found that free ZnPP did not produce any significant tumor accumulation at 24 h after intravenous injection, but nano or micellar forms of PSs showed markedly higher drug accumulation in various mouse and rat tumors, as shown by fluorescence imaging IVIS [65,66] (Figure 7A). In addition, these forms produced excellent antitumor effects in different xenograft mouse tumor models (e.g., mouse sarcoma S180, colon carcinoma C26, B16 melanoma) (Figure 7B) and AOM/DSS-induced autochthonous colon tumor in mice (Figure 4B) [10,27,28,66]. All the above findings suggest that nano-PSs have a potential for use in successful PDT for cancer by minimizing adverse effects.

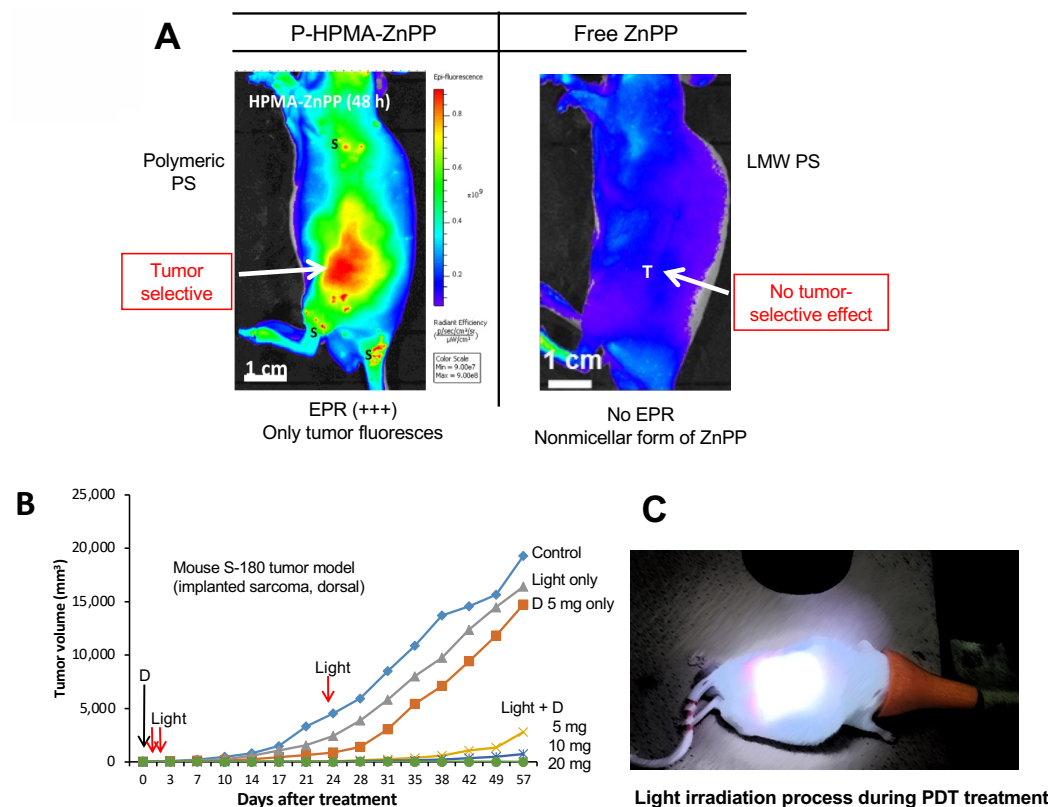


Figure 7. Advantages of EPR-based nano-sized photosensitizers (PSs) for PDT. When a macromolecular PS, PZP, was injected iv, intense drug accumulation occurred in the tumor after 24 h, as shown by IVIS fluorescence imaging (A, left image). In contrast, the LMW drug free ZnPP did not show any significant tumor drug accumulation (A, right image). (B) An excellent antitumor effect of PZP was seen in the mouse sarcoma S180 tumor model, especially with endoscopic light irradiation. “D” indicates the drug with iv PZP treatment; red arrows indicate light irradiation. (C) Light irradiation process with mouse tumor. Please see refs. [10,11,66].

12. Concluding Remarks

In this review, we described the rational and dynamic EPR effect, which was discovered by Professor Maeda and Dr. Matsumura in 1986 [6]. Some criticisms and arguments about the EPR-based tumor-selective accumulation of nanomedicines have appeared in the literature [45,46,49], but we and many other research groups throughout the world have addressed such misconceptions with considerable pre-clinical and clinical data [10,13,14,117–120]. One critical issue involves embolized or occluded tumor blood vessels, which lead to mistaken interpretations of the EPR effect [10]. To observe EPR-mediated tumor drug delivery, additional enhancement of tumor blood flow is necessary, because the EPR effect depends mainly on tumor blood flow [1,10]. We have discussed the various methods used to improve tumor blood flow, which Table 1 summarizes.

In addition, we have discussed the problems and solutions related to two important techniques in cancer treatment: BNCT and PDT. The advancement of these treatments in clinical settings is negligible because of the lack of active pharmaceutical ingredient entry into tumor tissue [11,65]. Nano formulations of borono-drugs or nano-PSs may be solutions for a successful strategy that utilizes BNCT and PDT for cancer treatment.

Author Contributions: This work was essentially designed by the late Professor Hiroshi Maeda. The manuscript was written primarily by T.S. and W.I. T.N., W.I. and T.S. discussed the content and refined the manuscript. All authors have read and agreed to the published version of the manuscript.

Funding: A part of this work was supported by the Japan Society for the Promotion of Science (a Postdoctoral Fellowship No. P21407) to WI and also by JST CREST (Grant Number JPMJCR18H5) to TN.

Institutional Review Board Statement: Not applicable.

Informed Consent Statement: Not applicable.

Data Availability Statement: Not applicable.

Acknowledgments: Fellowship: W. Islam is the recipient of a fellowship from the Japan Society for the Promotion of Science (JSPS) (2021–2023). English editing: We would like to acknowledge for important effort of MS Judith B. Gandy in AZ, USA for her excellent English editing.

Conflicts of Interest: The authors declare no conflict of interest.

References

1. Fang, J.; Nakamura, H.; Maeda, H. The EPR Effect: Unique Features of Tumor Blood Vessels for Drug Delivery, Factors Involved, and Limitations and Augmentation of the Effect. *Adv. Drug Deliv. Rev.* **2011**, *63*, 136–151. [[CrossRef](#)] [[PubMed](#)]
2. Golombek, S.K.; May, J.-N.; Theek, B.; Appold, L.; Drude, N.; Kiessling, F.; Lammers, T. Tumor Targeting via EPR: Strategies to Enhance Patient Responses. *Adv. Drug Deliv. Rev.* **2018**, *130*, 17–38. [[CrossRef](#)] [[PubMed](#)]
3. Maeda, H. Polymer Therapeutics and the EPR Effect. *J. Drug Target.* **2017**, *25*, 781–785. [[CrossRef](#)]
4. Maeda, H. Toward a Full Understanding of the EPR Effect in Primary and Metastatic Tumors as Well as Issues Related to Its Heterogeneity. *Adv. Drug Deliv. Rev.* **2015**, *91*, 3–6. [[CrossRef](#)]
5. Maeda, H.; Tsukigawa, K.; Fang, J. A Retrospective 30 Years After Discovery of the Enhanced Permeability and Retention Effect of Solid Tumors: Next-Generation Chemotherapeutics and Photodynamic Therapy—Problems, Solutions, and Prospects. *Microcirculation* **2016**, *23*, 173–182. [[CrossRef](#)] [[PubMed](#)]
6. Matsumura, Y.; Maeda, H. A New Concept for Macromolecular Therapeutics in Cancer Chemotherapy: Mechanism of Tumor-tropic Accumulation of Proteins and the Antitumor Agent Smancs. *Cancer Res.* **1986**, *46*, 6387–6392.
7. Fang, J.; Long, L.; Maeda, H. Enhancement of Tumor-Targeted Delivery of Bacteria with Nitroglycerin Involving Augmentation of the EPR Effect. *Methods Mol. Biol.* **2016**, *1409*, 9–23. [[CrossRef](#)]
8. Fang, J.; Sawa, T.; Maeda, H. Factors and Mechanism of “EPR” Effect and the Enhanced Antitumor Effects of Macromolecular Drugs Including SMANCS. *Adv. Exp. Med. Biol.* **2003**, *519*, 29–49. [[CrossRef](#)]
9. Folkman, J.; Klagsbrun, M. Angiogenic Factors. *Science* **1987**, *235*, 442–447. [[CrossRef](#)]
10. Fang, J.; Islam, W.; Maeda, H. Exploiting the Dynamics of the EPR Effect and Strategies to Improve the Therapeutic Effects of Nanomedicines by Using EPR Effect Enhancers. *Adv. Drug Deliv. Rev.* **2020**, *157*, 142–160. [[CrossRef](#)]
11. Maeda, H.; Islam, W. 3—Overcoming Barriers for Tumor-Targeted Drug Delivery: The Power of Macromolecular Anticancer Drugs with the EPR Effect and the Modulation of Vascular Physiology. In *Polymer-Protein Conjugates*; Pasut, G., Zalipsky, S., Eds.; Elsevier: Amsterdam, Netherlands, 2020; pp. 41–58; ISBN 978-0-444-64081-9.
12. Daruwalla, J.; Greish, K.; Malcontenti-Wilson, C.; Muralidharan, V.; Iyer, A.; Maeda, H.; Christophi, C. Styrene Maleic Acid-Pirarubicin Disrupts Tumor Microcirculation and Enhances the Permeability of Colorectal Liver Metastases. *J. Vasc. Res.* **2009**, *46*, 218–228. [[CrossRef](#)]
13. Lee, H.; Shields, A.F.; Siegel, B.A.; Miller, K.D.; Krop, I.; Ma, C.X.; LoRusso, P.M.; Munster, P.N.; Campbell, K.; Gaddy, D.F.; et al. ⁶⁴Cu-MM-302 Positron Emission Tomography Quantifies Variability of Enhanced Permeability and Retention of Nanoparticles in Relation to Treatment Response in Patients with Metastatic Breast Cancer. *Clin. Cancer Res.* **2017**, *23*, 4190–4202. [[CrossRef](#)] [[PubMed](#)]
14. Ding, Y.; Xu, Y.; Yang, W.; Niu, P.; Li, X.; Chen, Y.; Li, Z.; Liu, Y.; An, Y.; Liu, Y.; et al. Investigating the EPR Effect of Nanomedicines in Human Renal Tumors via Ex Vivo Perfusion Strategy. *Nano Today* **2020**, *35*, 100970. [[CrossRef](#)]
15. Duncan, R.; Sat-Klopsch, Y.-N.; Burger, A.M.; Bibby, M.C.; Fiebig, H.H.; Sausville, E.A. Validation of Tumour Models for Use in Anticancer Nanomedicine Evaluation: The EPR Effect and Cathepsin B-Mediated Drug Release Rate. *Cancer Chemother. Pharmacol.* **2013**, *72*, 417–427. [[CrossRef](#)] [[PubMed](#)]

16. Maeda, H. The 35th Anniversary of the Discovery of EPR Effect: A New Wave of Nanomedicines for Tumor-Targeted Drug Delivery—Personal Remarks and Future Prospects. *J. Pers. Med.* **2021**, *11*, 229. [[CrossRef](#)] [[PubMed](#)]
17. Maeda, H. Macromolecular Therapeutics in Cancer Treatment: The EPR Effect and Beyond. *J. Control. Release* **2012**, *164*, 138–144. [[CrossRef](#)] [[PubMed](#)]
18. MacConaill, L.E.; Campbell, C.D.; Kehoe, S.M.; Bass, A.J.; Hatton, C.; Niu, L.; Davis, M.; Yao, K.; Hanna, M.; Mondal, C.; et al. Profiling Critical Cancer Gene Mutations in Clinical Tumor Samples. *PLoS ONE* **2009**, *4*, e7887. [[CrossRef](#)]
19. Jiao, X.; Wei, X.; Li, S.; Liu, C.; Chen, H.; Gong, J.; Li, J.; Zhang, X.; Wang, X.; Peng, Z.; et al. A Genomic Mutation Signature Predicts the Clinical Outcomes of Immunotherapy and Characterizes Immunophenotypes in Gastrointestinal Cancer. *NPJ Precis. Oncol.* **2021**, *5*, 36. [[CrossRef](#)]
20. Fusco, M.J.; West, H.; Walko, C.M. Tumor Mutation Burden and Cancer Treatment. *JAMA Oncol.* **2021**, *7*, 316. [[CrossRef](#)]
21. Navi, B.B.; Reiner, A.S.; Kamel, H.; Iadecola, C.; Okin, P.M.; Tagawa, S.T.; Panageas, K.S.; DeAngelis, L.M. Arterial Thromboembolic Events Preceding the Diagnosis of Cancer in Older Persons. *Blood* **2019**, *133*, 781–789. [[CrossRef](#)]
22. Navi, B.B.; Reiner, A.S.; Kamel, H.; Iadecola, C.; Okin, P.M.; Elkind, M.S.V.; Panageas, K.S.; DeAngelis, L.M. Risk of Arterial Thromboembolism in Patients with Cancer. *J. Am. Coll. Cardiol.* **2017**, *70*, 926–938. [[CrossRef](#)]
23. Young, A.; Chapman, O.; Connor, C.; Poole, C.; Rose, P.; Kakkar, A.K. Thrombosis and Cancer. *Nat. Rev. Clin. Oncol.* **2012**, *9*, 437–449. [[CrossRef](#)]
24. Prabhakar, U.; Maeda, H.; Jain, R.K.; Sevic-Muraca, E.M.; Zamboni, W.; Farokhzad, O.C.; Barry, S.T.; Gabizon, A.; Grodzinski, P.; Blakey, D.C. Challenges and Key Considerations of the Enhanced Permeability and Retention (EPR) Effect for Nanomedicine Drug Delivery in Oncology. *Cancer Res.* **2013**, *73*, 2412. [[CrossRef](#)] [[PubMed](#)]
25. Tanaka, H.Y.; Kano, M.R. Stromal Barriers to Nanomedicine Penetration in the Pancreatic Tumor Microenvironment. *Cancer Sci.* **2018**, *109*, 2085–2092. [[CrossRef](#)]
26. Nel, A.; Ruoslahti, E.; Meng, H. New Insights into “Permeability” as in the Enhanced Permeability and Retention Effect of Cancer Nanotherapeutics. *ACS Nano* **2017**, *11*, 9567–9569. [[CrossRef](#)]
27. Seki, T.; Fang, J.; Maeda, H. Enhanced Delivery of Macromolecular Antitumor Drugs to Tumors by Nitroglycerin Application. *Cancer Sci.* **2009**, *100*, 2426–2430. [[CrossRef](#)]
28. Islam, W.; Fang, J.; Imamura, T.; Etrych, T.; Subr, V.; Ulbrich, K.; Maeda, H. Augmentation of the Enhanced Permeability and Retention Effect with Nitric Oxide-Generating Agents Improves the Therapeutic Effects of Nanomedicines. *Mol. Cancer Ther.* **2018**, *17*, 2643–2653. [[CrossRef](#)]
29. Islam, W.; Kimura, S.; Islam, R.; Harada, A.; Ono, K.; Fang, J.; Niidome, T.; Sawa, T.; Maeda, H. EPR-Effect Enhancers Strongly Potentiate Tumor-Targeted Delivery of Nanomedicines to Advanced Cancers: Further Extension to Enhancement of the Therapeutic Effect. *J. Pers. Med.* **2021**, *11*, 487. [[CrossRef](#)]
30. Fang, J.; Islam, R.; Islam, W.; Yin, H.; Subr, V.; Etrych, T.; Ulbrich, K.; Maeda, H. Augmentation of EPR Effect and Efficacy of Anticancer Nanomedicine by Carbon Monoxide Generating Agents. *Pharmaceutics* **2019**, *11*, 343. [[CrossRef](#)]
31. Fang, J.; Qin, H.; Seki, T.; Nakamura, H.; Tsukigawa, K.; Shin, T.; Maeda, H. Therapeutic Potential of Pegylated Hemin for Reactive Oxygen Species-Related Diseases via Induction of Heme Oxygenase-1: Results from a Rat Hepatic Ischemia/Reperfusion Injury Model. *J. Pharmacol. Exp. Ther.* **2011**, *339*, 779–789. [[CrossRef](#)] [[PubMed](#)]
32. Fang, J.; Qin, H.; Nakamura, H.; Tsukigawa, K.; Shin, T.; Maeda, H. Carbon Monoxide, Generated by Heme Oxygenase-1, Mediates the Enhanced Permeability and Retention Effect in Solid Tumors. *Cancer Sci.* **2012**, *103*, 535–541. [[CrossRef](#)]
33. Matsumoto, K.; Yamamoto, T.; Kamata, R.; Maeda, H. Pathogenesis of Serratia Infection: Activation of the Hageman Factor-Prekallikrein Cascade by Serratia Protease. *J. Biochem.* **1984**, *96*, 739–749. [[CrossRef](#)] [[PubMed](#)]
34. Maeda, H.; Yamamoto, T. Pathogenic Mechanisms Induced by Microbial Proteases in Microbial Infections. *Biol. Chem. Hoppe-Seyler* **1996**, *377*, 217–226. [[CrossRef](#)]
35. Molla, A.; Matsumura, Y.; Yamamoto, T.; Okamura, R.; Maeda, H. Pathogenic Capacity of Proteases from *Serratia Marcescens* and *Pseudomonas Aeruginosa* and Their Suppression by Chicken Egg White Ovomacroglobulin. *Infect. Immun.* **1987**, *55*, 2509–2517. [[CrossRef](#)]
36. Maeda, H.; Matsumura, Y.; Kato, H. Purification and Identification of [Hydroxypropyl³]Bradykinin in Ascitic Fluid from a Patient with Gastric Cancer. *J. Biol. Chem.* **1988**, *263*, 16051–16054. [[CrossRef](#)]
37. Matsumura, Y.; Maruo, K.; Kimura, M.; Yamamoto, T.; Konno, T.; Maeda, H. Kinin-Generating Cascade in Advanced Cancer Patients and in Vitro Study. *Jpn. J. Cancer Res.* **1991**, *82*, 732–741. [[CrossRef](#)]
38. Maeda, H.; Noguchi, Y.; Sato, K.; Akaike, T. Enhanced Vascular Permeability in Solid Tumor Is Mediated by Nitric Oxide and Inhibited by Both New Nitric Oxide Scavenger and Nitric Oxide Synthase Inhibitor. *Jpn. J. Cancer Res.* **1994**, *85*, 331–334. [[CrossRef](#)]
39. Maeda, H. SMANCS and Polymer-Conjugated Macromolecular Drugs: Advantages in Cancer Chemotherapy. *Adv. Drug Deliv. Rev.* **2001**, *46*, 169–185. [[CrossRef](#)]
40. Seymour, L.W.; Olliff, S.P.; Poole, C.J.; De Takats, P.G.; Orme, R.; Ferry, D.R.; Maeda, H.; Konno, T.; Kerr, D.J. A Novel Dosage Approach for Evaluation of SMANCS [Poly-(Styrene-Co-Maleyl-Half-n-Butylate)—Neocarzinostatin] in the Treatment of Primary Hepatocellular Carcinoma. *Int. J. Oncol.* **1998**, *12*, 1217–1223. [[CrossRef](#)]
41. Tsuchiya, K.; Uchida, T.; Kobayashi, M.; Maeda, H.; Konno, T.; Yamanaka, H. Tumor-Targeted Chemotherapy with SMANCS in Lipiodol for Renal Cell Carcinoma: Longer Survival with Larger Size Tumors. *Urology* **2000**, *55*, 495–500. [[CrossRef](#)]

42. Maeda, H. Principle and therapeutic effect of lipophilic anticancer agent [SMANCS/lipiodol]: Selective targeting with oily contrast medium. *Gan To Kagaku Ryoho* **1989**, *16*, 3323–3331.
43. Maeda, H. The Enhanced Permeability and Retention (EPR) Effect in Tumor Vasculature: The Key Role of Tumor-Selective Macromolecular Drug Targeting. *Adv. Enzyme Regul.* **2001**, *41*, 189–207. [[CrossRef](#)]
44. Maeda, H. Vascular Permeability in Cancer and Infection as Related to Macromolecular Drug Delivery, with Emphasis on the EPR Effect for Tumor-Selective Drug Targeting. *Proc. Jpn. Acad. Ser. B* **2012**, *88*, 53–71. [[CrossRef](#)]
45. Sindhvani, S.; Syed, A.M.; Ngai, J.; Kingston, B.R.; Maiorino, L.; Rothschild, J.; MacMillan, P.; Zhang, Y.; Rajesh, N.U.; Hoang, T.; et al. The Entry of Nanoparticles into Solid Tumours. *Nat. Mater.* **2020**, *19*, 566–575. [[CrossRef](#)]
46. Park, K. Questions on the Role of the EPR Effect in Tumor Targeting. *J. Control. Release* **2013**, *172*, 391. [[CrossRef](#)]
47. Nichols, J.W.; Bae, Y.H. EPR: Evidence and Fallacy. *J. Control. Release* **2014**, *190*, 451–464. [[CrossRef](#)] [[PubMed](#)]
48. Danhier, F. To Exploit the Tumor Microenvironment: Since the EPR Effect Fails in the Clinic, What Is the Future of Nanomedicine? *J. Control. Release* **2016**, *244*, 108–121. [[CrossRef](#)] [[PubMed](#)]
49. Kwon, I.K.; Lee, S.C.; Han, B.; Park, K. Analysis on the Current Status of Targeted Drug Delivery to Tumors. *J. Control. Release* **2012**, *164*, 108–114. [[CrossRef](#)] [[PubMed](#)]
50. Islam, W.; Fang, J.; Etrych, T.; Chytil, P.; Ulbrich, K.; Sakoguchi, A.; Kusakabe, K.; Maeda, H. HPMA Copolymer Conjugate with Pirarubicin: In Vitro and Ex Vivo Stability and Drug Release Study. *Int. J. Pharm.* **2018**, *536*, 108–115. [[CrossRef](#)] [[PubMed](#)]
51. Maeda, H.; Bharate, G.Y.; Daruwalla, J. Polymeric Drugs for Efficient Tumor-Targeted Drug Delivery Based on EPR-Effect. *Eur. J. Pharm. Biopharm.* **2009**, *71*, 409–419. [[CrossRef](#)]
52. Chytil, P.; Koziolová, E.; Etrych, T.; Ulbrich, K. HPMA Copolymer-Drug Conjugates with Controlled Tumor-Specific Drug Release. *Macromol. Biosci.* **2018**, *18*, 1700209. [[CrossRef](#)] [[PubMed](#)]
53. Peterson, C.M.; Shiah, J.-G.; Sun, Y.; Kopecková, P.; Minko, T.; Straight, R.C.; Kopecek, J. HPMA Copolymer Delivery of Chemotherapy and Photodynamic Therapy in Ovarian Cancer. *Adv. Exp. Med. Biol.* **2003**, *519*, 101–123. [[CrossRef](#)] [[PubMed](#)]
54. Ferreira, J.C.B.; Mochly-Rosen, D. Nitroglycerin Use in Myocardial Infarction Patients: Risks and Benefits. *Circ. J.* **2012**, *76*, 15–21. [[CrossRef](#)] [[PubMed](#)]
55. Mitchell, J.B.; Wink, D.A.; DeGraff, W.; Gamson, J.; Keefer, L.K.; Krishna, M.C. Hypoxic Mammalian Cell Radiosensitization by Nitric Oxide. *Cancer Res.* **1993**, *53*, 5845–5848. [[PubMed](#)]
56. Chen, Z.; Stamler, J.S. Bioactivation of Nitroglycerin by the Mitochondrial Aldehyde Dehydrogenase. *Trends Cardiovasc. Med.* **2006**, *16*, 259–265. [[CrossRef](#)] [[PubMed](#)]
57. Divakaran, S.; Loscalzo, J. The Role of Nitroglycerin and Other Nitrogen Oxides in Cardiovascular Therapeutics. *J. Am. Coll. Cardiol.* **2017**, *70*, 2393–2410. [[CrossRef](#)] [[PubMed](#)]
58. Pekarova, M.; Lojek, A.; Martiskova, H.; Vasicek, O.; Bino, L.; Klinke, A.; Lau, D.; Kuchta, R.; Kadlec, J.; Vrba, R.; et al. New Role for L-Arginine in Regulation of Inducible Nitric-Oxide-Synthase-Derived Superoxide Anion Production in Raw 264.7 Macrophages. *Sci. World J.* **2011**, *11*, 2443–2457. [[CrossRef](#)] [[PubMed](#)]
59. Akaike, T.; Maeda, H. Nitric Oxide and Virus Infection. *Immunology* **2000**, *101*, 300–308. [[CrossRef](#)] [[PubMed](#)]
60. Gladwin, M.T.; Shelhamer, J.H.; Ognibene, F.P.; Pease-Fye, M.E.; Nichols, J.S.; Link, B.; Patel, D.B.; Jankowski, M.A.; Pannell, L.K.; Schechter, A.N.; et al. Nitric Oxide Donor Properties of Hydroxyurea in Patients with Sickle Cell Disease. *Br. J. Haematol.* **2002**, *116*, 436–444. [[CrossRef](#)]
61. Sato, K.; Akaike, T.; Sawa, T.; Miyamoto, Y.; Suga, M.; Ando, M.; Maeda, H. Nitric Oxide Generation from Hydroxyurea via Copper-Catalyzed Peroxidation and Implications for Pharmacological Actions of Hydroxyurea. *Jpn. J. Cancer Res.* **1997**, *88*, 1199–1204. [[CrossRef](#)]
62. Mantle, J.A.; Russell, R.O.; Moraski, R.E.; Rackley, C.E. Isosorbide Dinitrate for the Relief of Severe Heart Failure after Myocardial Infarction. *Am. J. Cardiol.* **1976**, *37*, 263–268. [[CrossRef](#)]
63. Chavey, W.E.; Bleske, B.E.; Van Harrison, R.; Hogikyan, R.V.; Kesterson, S.K.; Nicklas, J.M. Pharmacologic Management of Heart Failure Caused by Systolic Dysfunction. *Am. Fam. Physician* **2008**, *77*, 957–964.
64. Nakamura, H.; Etrych, T.; Chytil, P.; Ohkubo, M.; Fang, J.; Ulbrich, K.; Maeda, H. Two Step Mechanisms of Tumor Selective Delivery of *N*-(2-Hydroxypropyl)Methacrylamide Copolymer Conjugated with Pirarubicin via an Acid-Cleavable Linkage. *J. Control. Release* **2014**, *174*, 81–87. [[CrossRef](#)]
65. Fang, J.; Šubr, V.; Islam, W.; Hackbarth, S.; Islam, R.; Etrych, T.; Ulbrich, K.; Maeda, H. *N*-(2-Hydroxypropyl)Methacrylamide Polymer Conjugated Pyropheophorbide-a, a Promising Tumor-Targeted Theranostic Probe for Photodynamic Therapy and Imaging. *Eur. J. Pharm. Biopharm.* **2018**, *130*, 165–176. [[CrossRef](#)]
66. Nakamura, H.; Liao, L.; Hitaka, Y.; Tsukigawa, K.; Subr, V.; Fang, J.; Ulbrich, K.; Maeda, H. Micelles of Zinc Protoporphyrin Conjugated to *N*-(2-Hydroxypropyl)Methacrylamide (HPMA) Copolymer for Imaging and Light-Induced Antitumor Effects in Vivo. *J. Control. Release* **2013**, *165*, 191–198. [[CrossRef](#)]
67. Saisyo, A.; Nakamura, H.; Fang, J.; Tsukigawa, K.; Greish, K.; Furukawa, H.; Maeda, H. PH-Sensitive Polymeric Cisplatin-Ion Complex with Styrene-Maleic Acid Copolymer Exhibits Tumor-Selective Drug Delivery and Antitumor Activity as a Result of the Enhanced Permeability and Retention Effect. *Colloids Surf. B* **2016**, *138*, 128–137. [[CrossRef](#)]
68. Islam, W.; Matsumoto, Y.; Fang, J.; Harada, A.; Niidome, T.; Ono, K.; Tsutsuki, H.; Sawa, T.; Imamura, T.; Sakurai, K.; et al. Polymer-Conjugated Glucosamine Complexed with Boric Acid Shows Tumor-Selective Accumulation and Simultaneous Inhibition of Glycolysis. *Biomaterials* **2020**, *269*, 120631. [[CrossRef](#)] [[PubMed](#)]

69. Fang, J.; Akaike, T.; Maeda, H. Antiapoptotic Role of Heme Oxygenase (HO) and the Potential of HO as a Target in Anticancer Treatment. *Apoptosis* **2004**, *9*, 27–35. [[CrossRef](#)] [[PubMed](#)]
70. Yin, H.; Fang, J.; Liao, L.; Nakamura, H.; Maeda, H. Styrene-Maleic Acid Copolymer-Encapsulated CORM2, a Water-Soluble Carbon Monoxide (CO) Donor with a Constant CO-Releasing Property, Exhibits Therapeutic Potential for Inflammatory Bowel Disease. *J. Control. Release* **2014**, *187*, 14–21. [[CrossRef](#)] [[PubMed](#)]
71. Seki, T.; Carroll, F.; Illingworth, S.; Green, N.; Cawood, R.; Bachtarzi, H.; Subr, V.; Fisher, K.D.; Seymour, L.W. Tumour Necrosis Factor-Alpha Increases Extravasation of Virus Particles into Tumour Tissue by Activating the Rho A/Rho Kinase Pathway. *J. Control. Release* **2011**, *156*, 381–389. [[CrossRef](#)]
72. du Vernay, A.J.V.B.; De Faveri, R.; Nunes, R.; Steimbach, V.M.B.; Santin, J.R.; Quintão, N.L.M. The Role of Kinins in the Proliferation of Fibroblast Primed with TNF in Scratch Wound Assay: Kinins and Cell Proliferation. *Int. Immunopharmacol.* **2018**, *65*, 23–28. [[CrossRef](#)]
73. Hisada, Y.; Ay, C.; Auriemma, A.C.; Cooley, B.C.; Mackman, N. Human Pancreatic Tumors Grown in Mice Release Tissue Factor-Positive Microvesicles That Increase Venous Clot Size. *J. Thromb. Haemost.* **2017**, *15*, 2208–2217. [[CrossRef](#)]
74. Tsumura, R.; Manabe, S.; Takashima, H.; Koga, Y.; Yasunaga, M.; Matsumura, Y. Evaluation of the Antitumor Mechanism of Antibody-drug Conjugates against Tissue Factor in Stroma-rich Allograft Models. *Cancer Sci.* **2019**, *110*, 3296–3305. [[CrossRef](#)]
75. Yasunaga, M.; Manabe, S.; Tsuji, A.; Furuta, M.; Ogata, K.; Koga, Y.; Saga, T.; Matsumura, Y. Development of Antibody-Drug Conjugates Using DDS and Molecular Imaging. *Bioengineering* **2017**, *4*, 78. [[CrossRef](#)]
76. Zhang, B.; Jiang, T.; She, X.; Shen, S.; Wang, S.; Deng, J.; Shi, W.; Mei, H.; Hu, Y.; Pang, Z.; et al. Fibrin Degradation by RtPA Enhances the Delivery of Nanotherapeutics to A549 Tumors in Nude Mice. *Biomaterials* **2016**, *96*, 63–71. [[CrossRef](#)] [[PubMed](#)]
77. Mei, T.; Shashni, B.; Maeda, H.; Nagasaki, Y. Fibrinolytic Tissue Plasminogen Activator Installed Redox-Active Nanoparticles (t-PA@iRNP) for Cancer Therapy. *Biomaterials* **2020**, *259*, 120290. [[CrossRef](#)]
78. Witte, L.; Hicklin, D.J.; Zhu, Z.; Pytowski, B.; Kotanides, H.; Rockwell, P.; Böhlen, P. Monoclonal Antibodies Targeting the VEGF Receptor-2 (Flk1/KDR) as an Anti-Angiogenic Therapeutic Strategy. *Cancer Metastasis Rev.* **1998**, *17*, 155–161. [[CrossRef](#)]
79. Jain, R.K. Normalization of Tumor Vasculature: An Emerging Concept in Antiangiogenic Therapy. *Science* **2005**, *307*, 58–62. [[CrossRef](#)]
80. Ikeda-Imafuku, M.; Wang, L.L.-W.; Rodrigues, D.; Shaha, S.; Zhao, Z.; Mitragotri, S. Strategies to Improve the EPR Effect: A Mechanistic Perspective and Clinical Translation. *J. Control. Release* **2022**, *345*, 512–536. [[CrossRef](#)]
81. Mattheolabakis, G.; Mikelis, C.M. Nanoparticle Delivery and Tumor Vascular Normalization: The Chicken or The Egg? *Front. Oncol.* **2019**, *9*, 1227. [[CrossRef](#)] [[PubMed](#)]
82. Chauhan, V.P.; Stylianopoulos, T.; Martin, J.D.; Popović, Z.; Chen, O.; Kamoun, W.S.; Bawendi, M.G.; Fukumura, D.; Jain, R.K. Normalization of Tumour Blood Vessels Improves the Delivery of Nanomedicines in a Size-Dependent Manner. *Nat. Nanotechnol.* **2012**, *7*, 383–388. [[CrossRef](#)]
83. Binnemars-Postma, K.A.; Ten Hoopen, H.W.; Storm, G.; Prakash, J. Differential Uptake of Nanoparticles by Human M1 and M2 Polarized Macrophages: Protein Corona as a Critical Determinant. *Nanomedicine* **2016**, *11*, 2889–2902. [[CrossRef](#)]
84. Maeda, H.; Nakamura, H.; Fang, J. The EPR Effect for Macromolecular Drug Delivery to Solid Tumors: Improvement of Tumor Uptake, Lowering of Systemic Toxicity, and Distinct Tumor Imaging in Vivo. *Adv. Drug Deliv. Rev.* **2013**, *65*, 71–79. [[CrossRef](#)] [[PubMed](#)]
85. Chauhan, V.P.; Martin, J.D.; Liu, H.; Lacorre, D.A.; Jain, S.R.; Kozin, S.V.; Stylianopoulos, T.; Mousa, A.S.; Han, X.; Adstamngkonkul, P.; et al. Angiotensin Inhibition Enhances Drug Delivery and Potentiates Chemotherapy by Decompressing Tumour Blood Vessels. *Nat. Commun.* **2013**, *4*, 2516. [[CrossRef](#)] [[PubMed](#)]
86. Wong, P.-P.; Demircioglu, F.; Ghazaly, E.; Alrawashdeh, W.; Stratford, M.R.L.; Scudamore, C.L.; Cereser, B.; Crnogorac-Jurcevic, T.; McDonald, S.; Elia, G.; et al. Dual-Action Combination Therapy Enhances Angiogenesis While Reducing Tumor Growth and Spread. *Cancer Cell* **2015**, *27*, 123–137. [[CrossRef](#)]
87. Mas-Moruno, C.; Rechenmacher, F.; Kessler, H. Cilengitide: The First Anti-Angiogenic Small Molecule Drug Candidate Design, Synthesis and Clinical Evaluation. *Anticancer Agents Med. Chem.* **2010**, *10*, 753–768. [[CrossRef](#)]
88. Ojha, T.; Pathak, V.; Shi, Y.; Hennink, W.E.; Moonen, C.T.W.; Storm, G.; Kiessling, F.; Lammers, T. Pharmacological and Physical Vessel Modulation Strategies to Improve EPR-Mediated Drug Targeting to Tumors. *Adv. Drug Deliv. Rev.* **2017**, *119*, 44–60. [[CrossRef](#)] [[PubMed](#)]
89. Kunjachan, S.; Kotb, S.; Pola, R.; Pechar, M.; Kumar, R.; Singh, B.; Gremse, F.; Taleeli, R.; Trichard, F.; Motto-Ros, V.; et al. Selective Priming of Tumor Blood Vessels by Radiation Therapy Enhances Nanodrug Delivery. *Sci. Rep.* **2019**, *9*, 15844. [[CrossRef](#)]
90. Lubner, M.G.; Brace, C.L.; Hinshaw, J.L.; Lee, F.T. Microwave Tumor Ablation: Mechanism of Action, Clinical Results and Devices. *J. Vas. Interv. Radiol.* **2010**, *21*, S192–S203. [[CrossRef](#)]
91. Kurokohchi, K.; Watanabe, S.; Masaki, T.; Hosomi, N.; Funaki, T.; Arima, K.; Yoshida, S.; Miyauchi, Y.; Kuriyama, S. Combined Use of Percutaneous Ethanol Injection and Radiofrequency Ablation for the Effective Treatment of Hepatocellular Carcinoma. *Int. J. Oncol.* **2002**, *21*, 841–846. [[CrossRef](#)]
92. Hijnen, N.M.; Heijman, E.; Köhler, M.O.; Ylihautala, M.; Ehnholm, G.J.; Simonetti, A.W.; Grüll, H. Tumour Hyperthermia and Ablation in Rats Using a Clinical MR-HIFU System Equipped with a Dedicated Small Animal Set-Up. *Int. J. Hyperth.* **2012**, *28*, 141–155. [[CrossRef](#)] [[PubMed](#)]

93. Lentacker, I.; De Cock, I.; Deckers, R.; De Smedt, S.C.; Moonen, C.T.W. Understanding Ultrasound Induced Sonoporation: Definitions and Underlying Mechanisms. *Adv. Drug Deliv. Rev.* **2014**, *72*, 49–64. [[CrossRef](#)]
94. Li, L.; Zhou, S.; Lv, N.; Zhen, Z.; Liu, T.; Gao, S.; Xie, J.; Ma, Q. Photosensitizer-Encapsulated Ferritins Mediate Photodynamic Therapy against Cancer-Associated Fibroblasts and Improve Tumor Accumulation of Nanoparticles. *Mol. Pharm.* **2018**, *15*, 3595–3599. [[CrossRef](#)] [[PubMed](#)]
95. Zhen, Z.; Tang, W.; Chuang, Y.-J.; Todd, T.; Zhang, W.; Lin, X.; Niu, G.; Liu, G.; Wang, L.; Pan, Z.; et al. Tumor Vasculature Targeted Photodynamic Therapy for Enhanced Delivery of Nanoparticles. *ACS Nano* **2014**, *8*, 6004–6013. [[CrossRef](#)] [[PubMed](#)]
96. Heber, E.M.; Hawthorne, M.F.; Kueffer, P.J.; Garabalino, M.A.; Thorp, S.I.; Pozzi, E.C.C.; Monti Hughes, A.; Maitz, C.A.; Jalisatgi, S.S.; Nigg, D.W.; et al. Therapeutic Efficacy of Boron Neutron Capture Therapy Mediated by Boron-Rich Liposomes for Oral Cancer in the Hamster Cheek Pouch Model. *Proc. Natl. Acad. Sci. USA* **2014**, *111*, 16077–16081. [[CrossRef](#)] [[PubMed](#)]
97. Rees, D.D.; Palmer, R.M.; Moncada, S. Role of Endothelium-Derived Nitric Oxide in the Regulation of Blood Pressure. *Proc. Natl. Acad. Sci. USA* **1989**, *86*, 3375–3378. [[CrossRef](#)]
98. Xu, W.; Liu, L.Z.; Loizidou, M.; Ahmed, M.; Charles, I.G. The Role of Nitric Oxide in Cancer. *Cell Res.* **2002**, *12*, 311–320. [[CrossRef](#)]
99. Fukumura, D.; Kashiwagi, S.; Jain, R.K. The Role of Nitric Oxide in Tumour Progression. *Nat. Rev. Cancer* **2006**, *6*, 521–534. [[CrossRef](#)] [[PubMed](#)]
100. Kamba, T.; McDonald, D.M. Mechanisms of Adverse Effects of Anti-VEGF Therapy for Cancer. *Br. J. Cancer* **2007**, *96*, 1788–1795. [[CrossRef](#)]
101. Bharadwaj, A.G.; Holloway, R.W.; Miller, V.A.; Waisman, D.M. Plasmin and Plasminogen System in the Tumor Microenvironment: Implications for Cancer Diagnosis, Prognosis, and Therapy. *Cancers* **2021**, *13*, 1838. [[CrossRef](#)]
102. Baig, M.U.; Bodle, J. Thrombolytic Therapy. In *StatPearls*; StatPearls Publishing: Treasure Island, FL, USA, 2022.
103. Barth, R.F. Boron Neutron Capture Therapy at the Crossroads: Challenges and Opportunities. *Appl. Radiat. Isot.* **2009**, *67*, S3–S6. [[CrossRef](#)] [[PubMed](#)]
104. Wang, S.; Zhang, Z.; Miao, L.; Li, Y. Boron Neutron Capture Therapy: Current Status and Challenges. *Front. Oncol.* **2022**, *12*, 788770. [[CrossRef](#)] [[PubMed](#)]
105. Koganei, H.; Ueno, M.; Tachikawa, S.; Tasaki, L.; Ban, H.S.; Suzuki, M.; Shiraishi, K.; Kawano, K.; Yokoyama, M.; Maitani, Y.; et al. Development of High Boron Content Liposomes and Their Promising Antitumor Effect for Neutron Capture Therapy of Cancers. *Bioconjugate Chem.* **2013**, *24*, 124–132. [[CrossRef](#)]
106. Kawasaki, R.; Sasaki, Y.; Akiyoshi, K. Self-Assembled Nanogels of Carborane-Bearing Polysaccharides for Boron Neutron Capture Therapy. *Chem. Lett.* **2017**, *46*, 513–515. [[CrossRef](#)]
107. Nedunchezian, K.; Aswath, N.; Thirupathy, M.; Thirugnanamurthy, S. Boron Neutron Capture Therapy—A Literature Review. *J. Clin. Diagn Res.* **2016**, *10*, ZE01–ZE04. [[CrossRef](#)]
108. Matsumoto, Y.; Fukumitsu, N.; Ishikawa, H.; Nakai, K.; Sakurai, H. A Critical Review of Radiation Therapy: From Particle Beam Therapy (Proton, Carbon, and BNCT) to Beyond. *J. Pers. Med.* **2021**, *11*, 825. [[CrossRef](#)]
109. Takano, S.; Islam, W.; Fujii, S.; Maeda, H.; Sakurai, K. Weak Interplay between Hydrophobic Part of Water-Soluble Polymers and Serum Protein. *Chem. Lett.* **2021**, *50*, 1392–1393. [[CrossRef](#)]
110. Pavlides, S.; Whitaker-Menezes, D.; Castello-Cros, R.; Flomenberg, N.; Witkiewicz, A.K.; Frank, P.G.; Casimiro, M.C.; Wang, C.; Fortina, P.; Addya, S.; et al. The Reverse Warburg Effect: Aerobic Glycolysis in Cancer Associated Fibroblasts and the Tumor Stroma. *Cell Cycle* **2009**, *8*, 3984–4001. [[CrossRef](#)]
111. Warburg, O. On the Origin of Cancer Cells. *Science* **1956**, *123*, 309–314. [[CrossRef](#)]
112. Dolmans, D.E.; Fukumura, D.; Jain, R.K. Photodynamic Therapy for Cancer. *Nat. Rev. Cancer* **2003**, *3*, 380–387. [[CrossRef](#)]
113. Wilson, B.C. Photodynamic Therapy for Cancer: Principles. *Can. J. Gastroenterol.* **2002**, *16*, 393–396. [[CrossRef](#)] [[PubMed](#)]
114. Baskaran, R.; Lee, J.; Yang, S.-G. Clinical Development of Photodynamic Agents and Therapeutic Applications. *Biomater. Res.* **2018**, *22*, 25. [[CrossRef](#)] [[PubMed](#)]
115. Nakamura, H.; Fang, J.; Gahininath, B.; Tsukigawa, K.; Maeda, H. Intracellular Uptake and Behavior of Two Types Zinc Protoporphyrin (ZnPP) Micelles, SMA-ZnPP and PEG-ZnPP as Anticancer Agents; Unique Intracellular Disintegration of SMA Micelles. *J. Control. Release* **2011**, *155*, 367–375. [[CrossRef](#)]
116. Fang, J.; Tsukigawa, K.; Liao, L.; Yin, H.; Eguchi, K.; Maeda, H. Styrene-Maleic Acid-Copolymer Conjugated Zinc Protoporphyrin as a Candidate Drug for Tumor-Targeted Therapy and Imaging. *J. Drug Target.* **2016**, *24*, 399–407. [[CrossRef](#)] [[PubMed](#)]
117. Abe, S.; Otsuki, M. Styrene Maleic Acid Neocarzinostatin Treatment for Hepatocellular Carcinoma. *Curr. Med. Chem. Anticancer Agents* **2002**, *2*, 715–726. [[CrossRef](#)]
118. Kubo, M.; Fuchigami, T.; Murata, S.; Konno, T.; Maeda, H. A case of massive hepatoma which responded to SMANCS/Lipiodol regimen with intra-arterial infusion. *Gan To Kagaku Ryoho* **1989**, *16*, 2953–2956.
119. Sakaguchi, T.; Yoshimatsu, S.; Sagara, K.; Yamashita, Y.; Takahashi, M. Intra-arterial infusion of SMANCS for treatment of patients with hepatocellular carcinoma—adverse reactions and complications. *Gan To Kagaku Ryoho* **1998**, *25* (Suppl. S1), 64–69.
120. Dozono, H.; Yanazume, S.; Nakamura, H.; Etrych, T.; Chytil, P.; Ulbrich, K.; Fang, J.; Arimura, T.; Douchi, T.; Kobayashi, H.; et al. HPMA Copolymer-Conjugated Pirarubicin in Multimodal Treatment of a Patient with Stage IV Prostate Cancer and Extensive Lung and Bone Metastases. *Target. Oncol.* **2016**, *11*, 101–106. [[CrossRef](#)]